International Journal of Applied Earth Observations and Geoinformation 112 (2022) 102856

Contents lists available at ScienceDirect

International Journal of Applied Earth Observations and Geoinformation

journal homepage: www.elsevier.com/locate/jag

Remote sensing image fusion on 3D scenarios: A review of applications for agriculture and forestry

Juan M. Jurado [a,*], Alfonso López [b], Luís Pádua [c], Joaquim J. Sousa [d,e]

[a] Department of Software Engineering. University of Granada. 18071 Granada, Spain
[b] Computer Graphics and Geomatics Group of Jaén. University of Jaén. 23071 Jaén, Spain
[c] Centre for the Research and Technology of Agro-Environmental and Biological Sciences (CITAB), Inov4Agro–Institute for Innovation, Capacity Building and Sustainability of Agri-Food Production, University of Trás-os-Montes and Alto Douro, 5000-801 Vila Real, Portugal
[d] Centre for Robotics in Industry and Intelligent Systems (CRIIS), INESC Technology and Science, 4200-465 Porto, Portugal
[e] University of Trás-os-Montes e Alto Douro, 5000-801 Vila Real, Portugal

ARTICLE INFO

Keywords:
Image Mapping
Data Fusion
3D Modeling
Survey

ABSTRACT

Three-dimensional (3D) image mapping of real-world scenarios has a great potential to provide the user with a more accurate scene understanding. This will enable, among others, unsupervised automatic sampling of meaningful material classes from the target area for adaptive semi-supervised deep learning techniques. This path is already being taken by the recent and fast-developing research in computational fields, however, some issues related to computationally expensive processes in the integration of multi-source sensing data remain. Recent studies focused on Earth observation and characterization are enhanced by the proliferation of Unmanned Aerial Vehicles (UAV) and sensors able to capture massive datasets with a high spatial resolution. In this scope, many approaches have been presented for 3D modeling, remote sensing, image processing and mapping, and multi-source data fusion. This survey aims to present a summary of previous work according to the most relevant contributions for the reconstruction and analysis of 3D models of real scenarios using multispectral, thermal and hyperspectral imagery. Surveyed applications are focused on agriculture and forestry since these fields concentrate most applications and are widely studied. Many challenges are currently being overcome by recent methods based on the reconstruction of multi-sensorial 3D scenarios. In parallel, the processing of large image datasets has recently been accelerated by General-Purpose Graphics Processing Unit (GPGPU) approaches that are also summarized in this work. Finally, as a conclusion, some open issues and future research directions are presented.

1. Introduction

Remote sensing data is rapidly increasing and many real-world scenarios are currently being replicated by the generation of virtual models in a three-dimensional (3D) space. The multi-source data integration and the 3D representation of surveyed areas is a hot research topic in the field of geoscience and remote sensing and has attracted the attention of both industry and academia (Ghamisi et al., 2019; Kotaridis and Lazaridou, 2021; Zhang et al., 2018). Focusing on natural and environmental areas, it has many prospective applications in smart agriculture (Jurado et al., 2020b; Pádua et al., 2019; Poblete et al., 2020, 2021), forestry and nature preservation (Almeida et al., 2021; Guimarães et al., 2020; Heckel et al., 2020; Schiefer et al., 2020) and monitoring (Maimaitijiang et al., 2020). Initially, the acquisition of remote sensing data required costly sensors mounted on complex platforms. Likewise, the surveying procedure and data processing were labor-intensive and time-consuming. Observed scenarios were mainly represented as bi-dimensional (2D) maps and orthophotos, after applying manual processes to correct the image distortion (Vong et al., 2021). In this field, significant advances have been achieved by the development of efficient methodologies for data acquisition and processing, as well as the production of new sensor capabilities and aerial platforms. Accordingly, intense research is currently being carried out focusing on multi-source data fusion and remote sensing image mapping on 3D models.

In recent years, huge datasets have been gathered for modeling and monitoring vegetation and environmental parameters aimed at the optimization of agroforestry activities. Many remote sensing techniques based on the use of specific sensors (LiDAR, RGB camera, multispectral,

* Corresponding author.
E-mail address: jjurado@ugr.es (J.M. Jurado).

https://doi.org/10.1016/j.jag.2022.102856
Received 20 February 2022; Received in revised form 21 May 2022; Accepted 1 June 2022
Available online 20 June 2022

thermal and hyperspectral) have been proposed to produce high-quality maps, orthomosaics and 3D models. In this context, the proliferation of Unmanned Aerial Vehicles (UAVs), as versatile and cost-efficient platforms to acquire multi-source data, enabled a detailed characterization of large scenarios, even with difficult accessibility. Undoubtedly, the UAV technology plays an important role in multidisciplinary research benefiting from unprecedented temporal, spatial and spectral resolutions of remote sensing data, acquired from multiple perspectives in a non-intrusive way.

The advancement of UAV-based sensors facilitates the development of remote sensing applications, such as early disease detection (Terentev et al., 2022), crop assessment (Ahmad et al., 2021; Chauhan et al., 2019), forest inventory (Pires et al., 2022), biomass estimation (Benson et al., 2021; Li et al., 2020b) and evaluation of natural disasters (Weiser et al., 2022). The use of UAVs for monitoring real-world scenarios also allows us to characterize them from multiple viewpoints by mounting different sensors. Current research aims to generate multi-source datasets and reveal hidden features that cannot be directly identified in data obtained from a single sensor. This research domain has also been motivated by the reconstruction of high-detailed 3D models to represent the shape and morphology of plants, terrain and other natural and artificial entities. Accordingly, their geometry and physiological traits can be studied jointly to provide a more accurate assessment of the plant cycle and environmental sustainability.

In parallel with the production of new UAV sensors, significant advances have been presented in data fusion and processing. In the last few years, large datasets are being collected for Earth observations by capturing high-resolution imagery that enables the generation of 3D models represented by dense point clouds. In this field, machine learning techniques are increasingly being used for 3D data applications such as crop classification (Jayakumari et al., 2021), tree species segmentation using LiDAR (Light Detection And Ranging) models and hyperspectral images (Mäyrä et al., 2021; Zhang et al., 2020), and assessing impacts of canopy 3D structure (Regaieg et al., 2021), among others. Undoubtedly, the combination of geometry and multi-source is crucial to improve machine learning-based studies which might incorporate multiple variables into the model (geometry, temperature, spectral reflectance, color, etc.). Accordingly, the fusion of remotely sensed images into 3D scenarios raises new developments based on image mapping to characterize the dynamic natural environment in terms of morphological and physiological features. Image mapping on 3D models aims to define the texture or color information onto the surface, which can be represented as point clouds or triangle meshes. Thus, thermal, multispectral and hyperspectral imagery can be mapped on 3D models that bring new opportunities for the digitalization and analysis of our environment. In contrast to 2D remote sensing monitoring, which has limitations for the detection of self-occluded vegetation areas, and the assessment of the canopy structure, 3D allows us to extract the height and volume of plants and to develop a more accurate analysis of the plant's condition considering geometric, spatial, and multi-temporal features. The use of 3D models in environmental, agriculture and forestry applications facilitate the individual recognition of trees, the study of spatial colonization by dominant species in natural environments, forest inventory, and harvest forecasting. Therefore, and considering the growing importance of 3D in the above-mentioned fields, in this work we describe the most significant advances in remote sensing image mapping on 3D scenarios. The main contributions of this paper can be summarized as:

- An overview, based on previous work of remote sensing techniques for image mapping on 3D scenarios, modeled from the real world. According to the data source, published works are classified into three categories: (1) thermal, (2) multispectral and (3) hyperspectral data. From this paper, readers can directly get a full picture of existing methods to obtain enriched 3D scenarios by using multi-source data.
- Description of main processes to represent sensing data on the 3D model, considering critical aspects such as occlusion issues, spatial resolution, performance and automation level.
- Review of the most used sensors and platforms for the acquisition of UAV-based imagery and 3D models.
- Presentation and discussion of main applications in the field of agriculture and forestry that benefit from the 3D representation of remote sensing datasets. For instance, 3D models can be used to retrieve multi-view information to help substantially improve the land cover mapping compared to the classification that only relies on 2D raster images.
- Highlighting open issues in the characterization of real-world environments by fusing geometric and semantic features on existing techniques for the representation of thermal, multispectral and hyperspectral data.

Table 1 summarizes previous surveys that cover similar research fields such where UAV-based remote sensing plays an important role. However, and different from the mentioned surveys, in this work we focus on multisensorial data fusion on 3D models. In addition, we present recent algorithms and their advantages for fusing 3D geometry and remote sensing imagery of natural environments. In summary, we present a compilation of a wide set of existing methods focused on studying not only the 3D reconstruction of real-world scenarios but also their combination with multispectral, thermal and hyperspectral imagery in forestry and agricultural applications.

This survey is organized as follows. In Section 2, the methodology that guided the bibliographic research carried out is presented. Section 3 provides a compendium of techniques for the acquisition and 3D reconstruction of real-world scenarios. Section 4 describes the main published works focused on fusing multispectral, thermal, and hyperspectral data with 3D models. Afterward, current applications and future trends are presented and discussed in Section 5. Finally, the main conclusions derived from this research domain are summarized and open research issues and future directions are pointed out in Section 6.

2. Methodology

The generation of three-dimensional models of real-world scenarios is increasingly common. However, most agricultural and forestry applications require parameters that are derived from aerial imagery obtained by RGB, multispectral, hyperspectral and thermal sensors. The

Table 1
A summary of other surveys that collect previous research where UAV-based remote sensing plays an important role.

Application	Surveys	Brief description
Forestry and agriculture	(Yandun Narvaez et al., 2017)	Ranging and Imaging Techniques for Precision Agriculture Phenotyping
	(Li et al., 2021)	Image fusion technology in agriculture
	(Tsouros et al., 2019)	UAV-Based Applications for Precision Agriculture
	(Guimarães et al., 2020)	Forestry Remote Sensing from Unmanned Aerial Vehicles
3D modeling and mapping	(Iglhaut et al., 2019)	UAV for 3D mapping applications.
	(Jiang et al., 2020)	Efficient structure from motion for large-scale UAV images.
	(Yao et al., 2019)	Unmanned Aerial Vehicle for Remote Sensing Applications
Data fusion	(Ghamisi et al., 2019)	Multisource and Multitemporal Data Fusion in Remote Sensing
	(Paul and Pati, 2021)	A comprehensive review on remote sensing image registration
Remote sensing image fusion on 3D models	Our survey	Integration of multi-source UAV imagery on 3D models.

combination of these multisensorial data with the 3D geometry of both natural and artificial entities brings a deep knowledge of our environment.

Three-dimensional modeling applied to several remote sensing devices covers the methodology for generating 3D scenarios with any geometrical description while also integrating a specific data source. Thus, this review is not solely focused on 3D environments described through point clouds of meshes. To provide a relevant description of the state-of-the-art concerning remote sensing data fusion in 3D scenarios, we explore previous research related to the most relevant remote sensing data sources. In this work, we aim to collect existing methodologies applied to visible, thermal, multispectral and hyperspectral imagery. It is also intended, for this review, to describe the most common approaches related to the reconstruction of 3D environments, such as photogrammetric techniques, as well as enhancements of such methods and alternatives to conventional approaches, whether they can be applied to small or large datasets. Therefore, a review regarding their applicability to frequent surveying techniques, such as UAV flights, is also provided. Despite the growing interest in 3D modeling in recent years, some of the above data sources remain unexplored. This phenomenon is even more noticeable in natural environments, although some data sources have been successfully applied to other fields. Hence, we intend to provide the basis to build 3D models for agriculture and forestry, instead of only exploring existing works concerning our area of interest.

A wide variety of research was reviewed in this study, using Scopus as the main cross-library search tool. Regarding multispectral, thermal, and hyperspectral modeling, the search was performed by the title, abstract and keywords, using the following term combination: "3D AND point AND cloud AND thermal". For other imagery sources, the term "thermal" was exchanged by the corresponding source, i.e., "multispectral" and "hyperspectral". This query produced 245 results for 3D thermal modeling, from which a total of 62 articles were finally selected in our review according to their relevance and concordance to the topic of this survey. Concerning 3D multispectral image mapping, the query returned 224 results, from which 85 were finally cited. Regarding hyperspectral data, the number of available studies drops dramatically (116 results). On the one hand, this is a field where major developments are now taking place, on the other hand, access to this type of technology remains very expensive and, finally, the resources needed to process and analyze this data are still under development. Due to the high number of existing research in this domain, one of the main challenges of this survey is to synthesize a selection of all those papers whose contribution to the remote sensing image fusion on 3D scenarios is significantly relevant after a careful review. Fig. 1 shows the weight of publications in the top-6 scientific journals in this field.

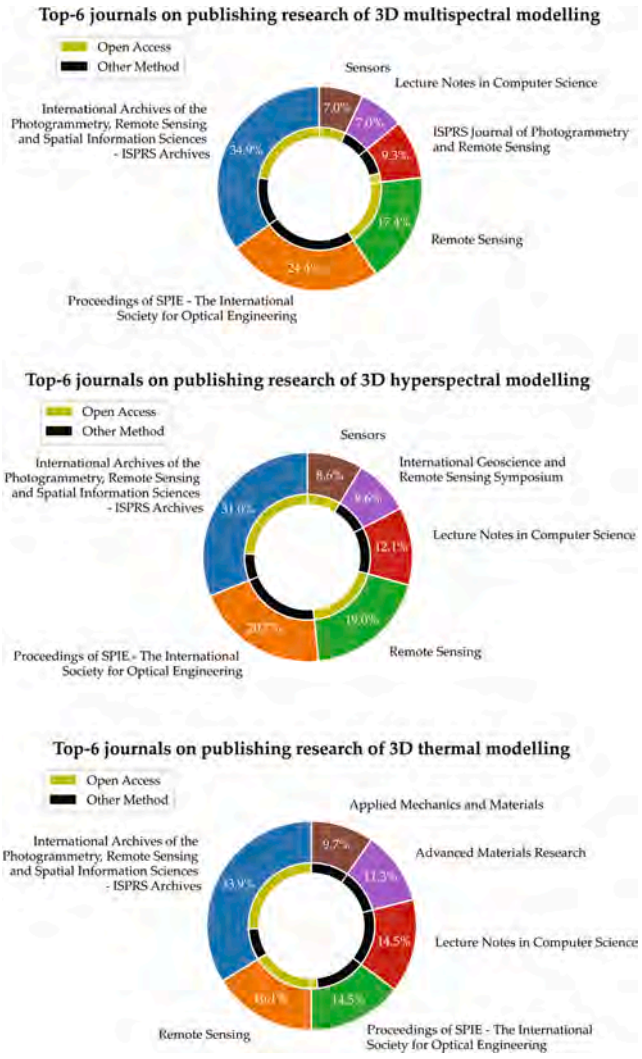

Fig. 1. Summary of the six most representative journals publishing work related to 3D point clouds concerning multispectral, hyperspectral and thermal data sources. To this aim, we performed a Scopus search using the keywords '3D AND point AND cloud', appending the objective data source at the end of the title query. Along with the journal title, the publication method is also depicted.

3. The 3D reconstruction of real scenarios

Three-dimensional representation of real-world scenarios has enjoyed a great interest to improve visualization and interpretation of the surveyed areas and phenomena. However, important limitations arise with data acquisition and monitoring processes in natural scenarios. The acquired images have a strong dependency on the angle and position of the camera or sensor. In fact, some areas are not visible because they are self-hidden from the nadir view angle, especially the lower structures. To solve these issues, 3D point clouds and imaging-based sensors are combined, allowing to retrieve heterogeneous information of the whole model. Together, geometry and multi-sensor data of the surveyed area, provide a complete information system for a detailed analysis of natural and urban environments.

A wide variety of sensors has burst onto the market for capturing the three-dimensional nature of the environment, whether natural or urban. Some examples of these acquisition technologies and methods are Radio Detection And Ranging (RaDAR) (Feng et al., 2016), Light Detection and Ranging (LiDAR) (Su et al., 2016) and structure-from-motion (SfM) (Rahlf et al., 2017). As shown in Fig. 2, several 3D modeling techniques can be performed following image-based approaches and either terrestrial or aerial LiDAR scans. Regardless of the method used, the result is a georeferenced point cloud with additional information such as the RGB color of the area representing each of these points.

3D point clouds are commonly used to represent complex surfaces of the real world. In contrast to 3D meshes, they enable a simpler, denser and more close-to-reality representation (Cao et al., 2019). These models are generated to represent both static and dynamic 3D objects, which are characterized by dense geometric data and other attributes. The latter features are obtained by fusing point clouds with other sensing data such as multispectral, hyperspectral or thermal images. To this end, both point clouds and multi-source images are processed together to map relevant image-based characteristics for each 3D point. Reviewing the scientific literature, it can be concluded that this problem is similar to that posed in the technique called projective texture mapping (Debevec et al., 1998; Everitt, 2001; Heckbert, 1986). Initially, the aim was to have additional effects on the realistic image synthesis field of research, to cast shadows or render translucent objects (Dachsbacher and Stamminger, 2003).

This process poses a prevalent challenge in the current scenario,

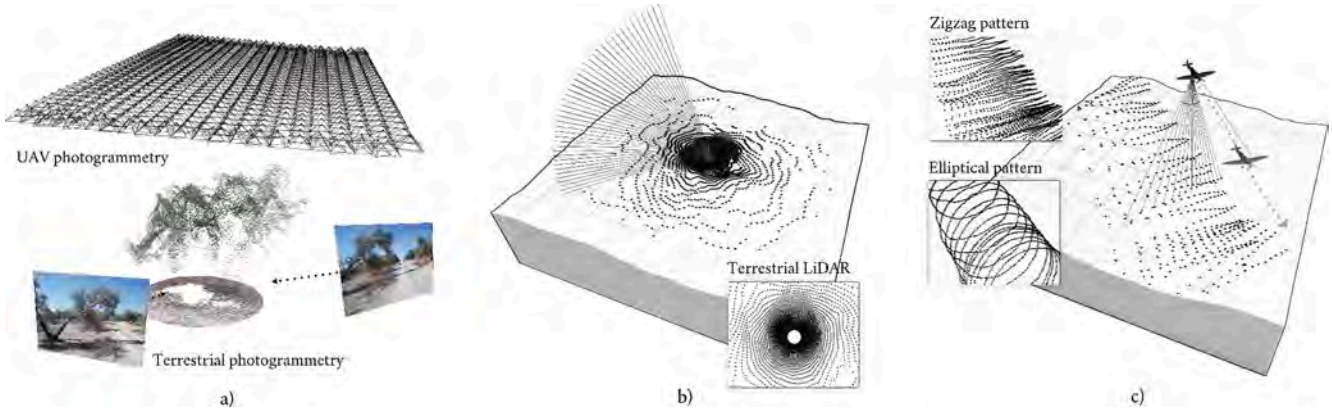

Fig. 2. Graphical scheme summarizing 3D modeling methodologies and expected results. (a) Image-based techniques for the 3D reconstruction by terrestrial and aerial photogrammetry, (b) terrestrial-LiDAR techniques, and (c) aerial-LiDAR modeling.

considering the high number of high-resolution images and the huge amount of 3D points in the cloud - several hundred million can easily be achieved. These requirements led to the development and/or improvement of computational and storage capabilities, databases and true collaborative environments. Consequently, tools based on 3D data processing and analysis are rapidly increasing to enhance multidisciplinary research. The visualization and interaction with detailed 3D models should ensure real-time feedback for collaborative tasks. Therefore, efficient methods must be developed in order to exploit the hardware capabilities and ensure high performance. Thus, experts from different disciplines can collaborate on 3D environments which are user-friendly. To deal with the challenge of processing huge amounts of input data from different sources, general-purpose computing on graphics processing units (GPGPU) techniques are used to take advantage of parallel and distributed computing strategies. In contrast to classical sequential methods, the computational resources offered by graphics processing unit (GPU) devices suppose a great opportunity to accelerate image-based operations, 3D projections, geometric transformations, and occlusion tests (López et al., 2021c).

Massive data processing is a trend that arouses the interest of multidisciplinary research since it allows accelerating large processing tasks. Some examples of this are feature matching of UAV imagery or any subsequent processing concerning large 3D point clouds, such as the occlusion detection, normal vector estimation, or their rendering to an image. However, there are still many limitations that should be addressed. GPGPU algorithms perform compute-intensive tasks, though they are also constrained by limited memory resources and high latency of data transfers between the central processing unit (CPU) and GPU. Nevertheless, new strategies are highly demanded to ensure not only fast methods but also the processing of large datasets.

4. Remote sensing image processing and 3D mapping

Nowadays, Remote Sensing is a hot research topic in terms of applicability and use cases, because of the large availability of remote-sensed datasets based on satellites and UAVs. Accordingly, high active and multidisciplinary research is being developed and many scientists aim to get advantages from the efficient acquisition methodologies for monitoring and evaluating real-world scenarios.

The integration of multi-source imagery in combination with 3D reconstructed scenarios is still challenging since each dataset has different features related to the acquisition system (global or rolling shutter, push-broom sensors, etc.), intrinsic and extrinsic parameters, model image distortion and image resolution. Hence, heterogeneous datasets can be acquired but mapping them on 3D models is not a trivial task. Moreover, operations with large sets of images and dense geometry arise from high computational efforts, which may be accelerated with parallel computation. In the following subsections, the main contributions in the field of remote sensing image mapping on 3D models are summarized. For this purpose, three types of images widely used in remote sensing are considered: multispectral, thermal and hyperspectral imagery. A general overview of the most used techniques for processing and 3D modeling from multispectral, thermal and hyperspectral images is presented in Fig. 3. Likewise, Table 2 summarizes a selection of papers considering the data source and procedures for the integration with 3D models.

4.1. Multispectral imagery

In the last decade, the proliferation of low-cost multispectral sensors led to the capture of massive multispectral data for different applications such as agriculture (Deng et al., 2018a; Pádua et al., 2019; Poblete et al., 2020), forestry and ecology (Dalponte et al., 2020; Guimarães et al., 2020; Schiefer et al., 2020; Torresan et al., 2017). More recently, deep learning techniques are also being explored in this type of data (Correa et al., 2020; Rapaka and Ramu, 2021, 2021; Yu et al., 2021). In the field of forestry and agriculture, recent advances have been proposed for multi-temporal monitoring (Du et al., 2020; Ghamisi et al., 2019; Jurado et al., 2020b; Pádua et al., 2020) and semantic segmentation (Gani et al., 2021; Jurado et al., 2020a; Qiu et al., 2020; Wan et al., 2021, 2021; Zhang et al., 2020). Multispectral sensors provide a limited number of narrow spectral bands, from which key plant-light interactions can be observed and many physiological parameters can be extracted and analyzed. In contrast to hyperspectral sensors described in Section 4.3, multispectral data only represents some meaningful spectral bands that are mainly used to monitor crops, soil and natural resources (López et al., 2021a). Moreover, spectral bands can be combined to compute spectral indices, such as Normalized Difference Vegetation Index (NDVI), Normalized Difference Water Index (NDWI), Normalized Pigment Chlorophyll Ratio Index (NPCRI), among others. Over years many spectral indices have been introduced by the scientific community to assess complex environmental issues (Mesas-Carrascosa et al., 2020; Pôças et al., 2020; Zhang et al., 2021).

The generation of 3D multispectral data is possible due to a high increase in image quality and resolution provided by recent acquisition systems. The 3D representation of reflectance distribution along the model surface allows us to develop a more detailed inspection and analysis of plant health. Thus, self-occluded features can be revealed by being observed from multiple viewpoints and represented on a 3D model. According to previous studies focused on the 3D reconstruction of multispectral imagery, in this survey two main categories are described considering the data acquisition system: satellite-based and UAV-based imagery. Fig. 4 shows multispectral datasets, their corresponding data sources and a plausible 3D model of a forest. Both types of

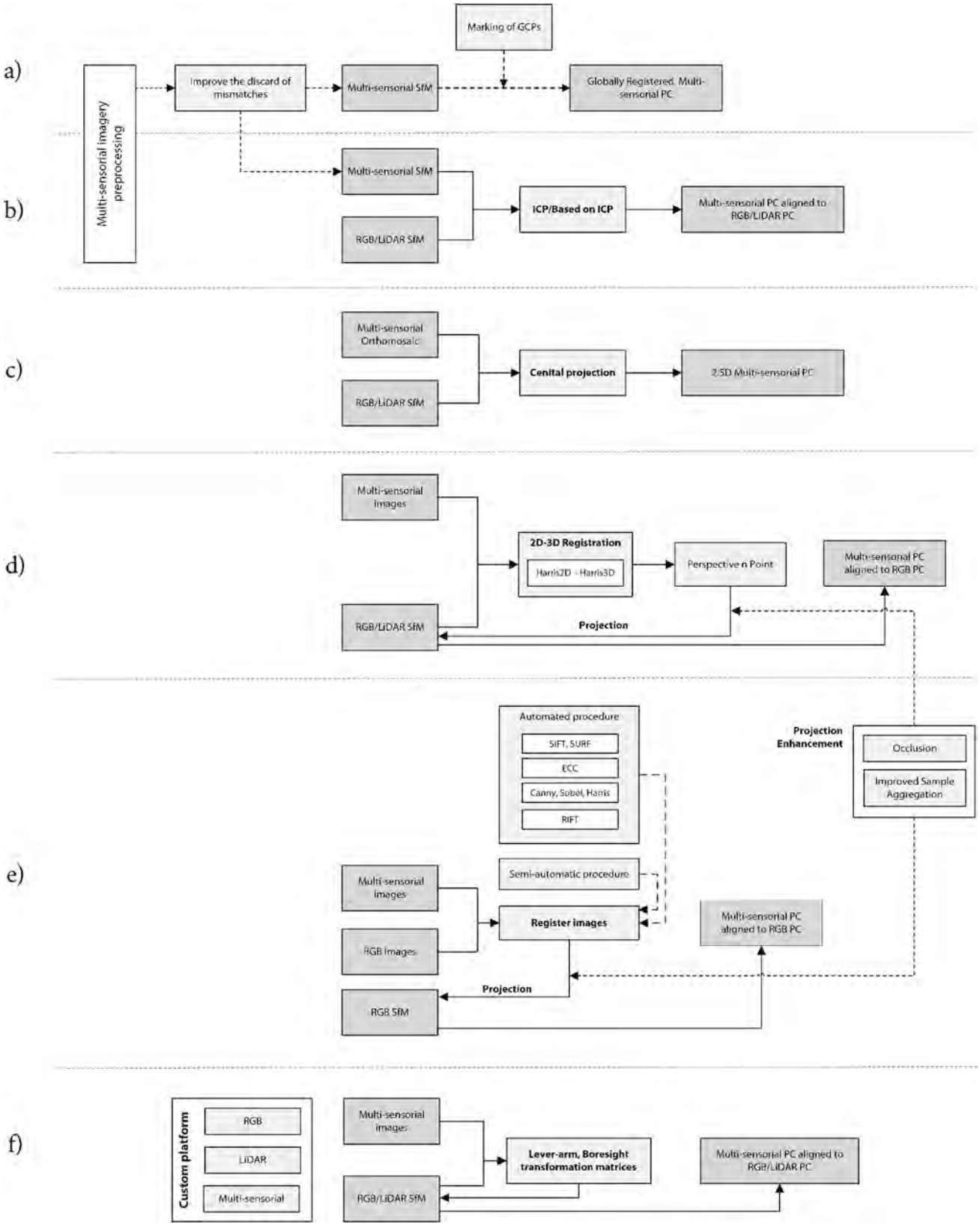

Fig. 3. Workflow of main procedures observed in the literature for 3D modeling using multispectral, thermal and hyperspectral images. Dotted lines represent optional steps for improving the core algorithm. The mapping categories are summarized as follows: a) the 3D reconstruction is solely based on the SfM algorithm using images of the relevant sensor, b) a base point cloud is aligned with an alternative point cloud, in order to increase the positioning accuracy, c) a 2.5D point cloud is generated using a base point cloud and the orthomosaic of an alternative data source, d) images are mapped into the base point cloud once 2D and 3D features are identified and used to estimate pose parameters, e) features are sought in 2D to compute the transformation matrix between RGB and an alternative data source, and f) a new approach, considering sensors previously calibrated, with the aim of projecting multi-sensorial images on the point cloud. The term GCP refers to Ground Control Points, i.e., georeferenced points aimed at enhancing the precision of resulting point clouds.

Table 2
Relevant papers for building a 3D multispectral, hyperspectral or thermal point cloud, using the methodology classification depicted in Fig. 3.

Data source	Methodology					
	a) SfM	b) SfM and ICP	c) Orthomosaic Projection (2.5D)	d) Registration of 2D and 3D features	e) Image registration	f) Inter-sensor calibration
Multispectral	(Jiang et al., 2020; Villacrés and Auat Cheein, 2022)	(Clamens et al., 2021; Jurado et al., 2020b, 2020a, 2020c)	(Comba et al., 2018; Matese et al., 2017; Shen et al., 2019)	(Clamens et al., 2021; Gui and Qin, 2021; Liu et al., 2018)	(Maimaitijiang et al., 2020; Ruiz et al., 2019; Tsai and Lin, 2017)	(Gu et al., 2020; Manzanera et al., 2016; Sankey et al., 2021; Valbuena et al., 2018)
Thermal	(Dahaghin et al., 2021; González et al., 2019; Grechi et al., 2021; Guilbert et al., 2020; Jeong et al., 2021; Zheng et al., 2020)	(Hoegner and Stilla, 2018; Lin et al., 2019a; Maset et al., 2017; Webster et al., 2018)	(Adán et al., 2020; Lorenzo Comba et al., 2019)	(Lin et al., 2019a; Zhu et al., 2019, 2021)	(Hoegner et al., 2016b; Huang et al., 2018; Javadnejad et al., 2020; Landmann et al., 2019; Lin et al., 2019a; López et al., 2021b; Macher et al., 2019)	(Adán et al., 2017; Dino et al., 2020; Hoegner et al., 2018; Javadnejad et al., 2020; Landmann et al., 2019)
Hyperspectral	(Aasen et al., 2015; Cao et al., 2018; Näsi et al., 2018, 2015; Sothe et al., 2019; Yue et al., 2018)	–	(Li et al., 2020a; Nezami et al., 2020)	–	(Angel et al., 2020; Fang et al., 2019; Jurado et al., 2021)	(Almeida et al., 2021; Lin et al., 2019a; Sankey et al., 2017, 2018)

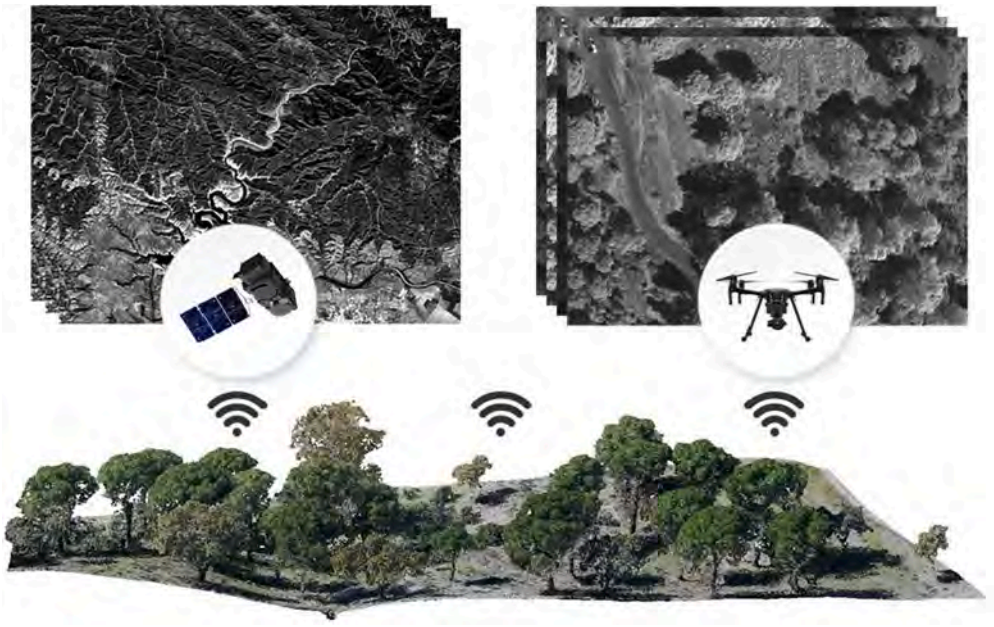

Fig. 4. Comparison of satellite multispectral images (GSD: 10 m) from Sentinel-2 mission and UAV-based multispectral imagery (GSD: 3 cm). The UAV-based multispectral sensor captures four bands, whereas the satellite provides ten spectral bands. Both images show a mountain area in Jaén, Spain. This area is represented by a photogrammetric point cloud.

imagery are extensively used by scientists and each one raises advantages but also limitations. Main techniques and popular sensors are reviewed to pose a general overview of existing solutions for the generation of 3D multispectral models.

The availability of high spatial resolution and multitemporal imagery from satellites allows for monitoring large-scale scenarios of the real world. These images can be obtained from different satellites of American Landsat programs, Copernicus missions (Main-Knorn et al., 2017; Wulder et al., 2019) and other private projects (Airbus, Kompsat, SuperWill, Pléiades, etc.) (Effiom et al., 2019; Lee et al., 2020). For instance, the spectral resolution of Sentinel-2 (Copernicus program) is determined by thirteen spectral bands, four of them with the highest spatial resolution (10 m) in the visible and near-infrared (VNIR) range. A lower spatial resolution is presented for other bands in short-wave infrared (SWIR) ranges (20 m−60 m). According to multispectral imagery generated by Landsat 8–9, nine spectral bands with a spatial resolution of 30 m are provided. A higher image resolution is achieved by other satellites such as Pléiades 1 or Kompsat 3, with a Ground Sample Distance (GSD) of approximately 2.8 m/px.

Traditionally, most of the previous work is based on satellite image mapping on 3D photogrammetric point clouds and LiDAR models for monitoring the forest structure (Bolton et al., 2020; Lechner et al., 2020), multitemporal observation of crops (Gadiraju et al., 2020; Qadeer et al., 2021) and semantic segmentation of urban and natural scenarios (Ballouch et al., 2022; Saralioglu and Gungor, 2020). State-of-the-art reconstruction methods from satellite data typically generate elevation data. Over the last few years, promising studies have focused on the super-resolution of satellite images through different deep learning approaches (Gómez et al., 2022; Keshk and Yin, 2017; Müller et al., 2020; Nguyen et al., 2021; Rohith and Kumar, 2020; Stucker and Schindler, 2022). Consequently, the cited advances and modern high-resolution satellite sensors allow us to recover full 3D surfaces from multi-view satellite panchromatic images (Han et al., 2020; Rothermel et al., 2020; Rupnik et al., 2018). Digital surface models can be efficiently modeled with automatic image matching from multiple optical stereo images, which are acquired in the same orbit (Gui and Qin, 2021;

Qin, 2019). The resulting 3D meshes or point clouds can be directly fused with multispectral bands of satellite imagery. According to the satellite's capabilities to produce 3D multispectral data, the most recent studies only produce digital elevation models (DEM) enriched by spectral attributes to enable a more comprehensive characterization and view of the surveyed area (Dalponte et al., 2020; Sagan et al., 2021; Wang and Li, 2020). Thus, real-world 3D scenarios can be labeled and this data provides a high interest for many environmental applications. In fact, to increase the size of current multispectral satellite image sets, recent work is focused on Generative Adversarial Networks (GANs) for the generation of synthetic multispectral satellite images (Abady et al., 2020; Mohandoss et al., 2020). These techniques allow obtaining labeled synthetic imagery that can be mapped on 3D scenarios in data-scarce regions.

Recently, novel aerial platforms and multispectral sensors are emerging in order to increase the accuracy of spectral measurements, reduce the noise coming from different layers of the atmosphere, and increase the model coverage by multiple view-points with a higher spatial resolution (Deng et al., 2018a). The UAV's capabilities to carry lightweight imaging systems have positively impacted recent research. To date, a wide range of multispectral sensors has been produced as summarized in Table 3. In contrast to satellite images, the GSD of UAV-multispectral imagery can be significantly reduced to ~ 2 cm/px by planning a flight of 30 m height. The increase in spatial resolution and the possibility to capture many overlapped images enable the development of image-based techniques for 3D model reconstruction. In the following, according to the sensor's features and proposed methodologies, a brief description of previous work and preliminary results are presented.

Digital surface modeling may be performed by UAV photogrammetric reconstruction using multispectral imagery. James et al. (2021) highlighted the contribution of infrared channels (NiR and Red-Edge) compared to the visible ones for the XYZ accuracy in the digital surface model (DSM) reconstruction over the coastal fringe. 3D points are usually reconstructed using images in every single spectral band. Speeded up robust features (SURF) algorithms (Oyallon and Rabin, 2015; Sedaghat and Mohammadi, 2019) and Scale-invariant feature transform (SIFT) algorithms (Saleem and Sablatnig, 2014) are commonly applied for feature detection and feature matching. According to previous studies that summarized the results of aerial image registration (Tsai and Lin, 2017), the SIFT method outperformed other algorithms in terms of quality of results and runtime. In this scope, Matese et al. (2017) presented an assessment of the canopy height model in a vineyard using UAV-based multispectral imaging, Liu et al. (2018) proposed a method for multispectral 3D points registration and plant inspection and Zainuddin et al. (2019) discussed the multispectral camera capabilities to acquire 3D data. The extracted tie points were generated using SfM, which were then used as input to generate a dense point cloud based on the multi-view stereo (MVS).

Although UAV multispectral images have enough resolution to directly generate photogrammetric point clouds, which may be upsampled later (Qian et al., 2021), other work is focused on multispectral image mapping on 3D models, which can be generated by using LiDAR sensors or RGB imagery. In the following paragraphs, recent work is presented considering: (1) image-based methods, and (2) LiDAR-based solutions for the generation of 3D multispectral data. Recently, Jurado et al. (2020b) proposed a novel pipeline to generate dense multispectral point clouds by mapping multispectral images on dense point clouds which were reconstructed using high-resolution RGB images. Firstly, a sparse point cloud is reconstructed using NIR images. This 3D model is then aligned with the RGB model and the resulting transformation is applied for each multispectral camera. Thus, a unique reference system is set and then, every multispectral image is mapped on the RGB point cloud considering the occlusion problem. Since multispectral images have a lower resolution than RGB images, the K-Nearest Neighbor algorithm is used for resampling to obtain spatially matched multispectral and RGB 3D models. With this solution, dense point clouds with multispectral attributes can be generated. Other studies focused on generating multispectral point clouds by digital aerial photogrammetry. Comba et al. (2018) used the exact detection of vineyards from 3D point-cloud maps, generated from UAV multispectral imagery. Shen et al. (2019) generated point clouds from UAV multispectral and RGB images

Table 3
List of the most used multispectral sensors available for being coupled with UAVs.

Manuf.	Sensor	Spectral bands, center and bandwidth (nm)	HFOV	GSD@120 m (cm)	Weight (gr)	Research articles
Parrot	Sequoia	Green: 550 (40) Red: 660 (40) Red-edge: 735 (10) Near-IR: 790 (40)	63.9°	8	135	(Franzini et al., 2019)
Micasense	RedEdge-MX	Blue: 475 (32) Green: 560 (27) Red: 668 (14) Red edge: 717 (12) Near-IR: 842 (57)	47.2°	3.4	180	(Cunha et al., 2021; Isgró et al., 2021)
Micasense	Dual-camera system	Coast blue: 444 (28) Blue: 475 (32) Green 1: 531 (14) Green 2: 560 (27) Red 1: 650 (16) Red 2: 668 (14) Red-edge 1: 705 (10) Red-edge 2: 717 (12) Red-edge 3: 740 (18) Near-IR: 842 (57)	47.2°	3.4	508.8	(Chakhvashvili et al., 2021)
Micasense	Altum	Blue: 475 (32) Green: 560 (27) Red: 668 (14) Red-edge: 717 (12) Near-IR: 842 (57) LWIR: 11 (6) μm	48°	5.2	357	(Hutton et al., 2020)
DJI	P4 Multispectral	Blue: 450 (16) Green: 560 (16) Red: 650 (16) Red-edge: 730 (16) Near-IR: 840 (26)	62.7°	6.3	1487	(Lu et al., 2020)

for the estimation of forest structural attributes. Villacrés et al. (2022) proposed the reconstruction of 3D maps of vegetation indices retrieved from UAV multispectral imagery in forested areas. Moreover, other approaches are based on multispectral image registration on 3D point clouds using RGB-D sensors that can be embedded on aerial and terrestrial platforms. Clamens et al. (2021) implemented a method based on feature-based and corner-based registration approaches to register images from the RGB-D camera with multispectral images. The combination of multispectral, RGB and depth images generates a multi-modal data fusion, which allows the extraction of several types of information from the environment.

Regarding other studies that use multispectral 3D data, the integration of LiDAR and multispectral sensors is a well-known solution. Initially, these acquisition systems were quite heavy and coupled to an aircraft. Previous work was developed for forest structure characterization (Manzanera et al., 2016) and urban scene classification (Guo et al., 2011). Data fusion was carried out by the back-projection method, proposed by Valbuena et al. (2014). Back-projecting consists in rendering LiDAR from the optical camera's perspective to obtain the pixel information that corresponds to each return. Then, the pixel attributes are fetched and retrieved to the original position of LiDAR returns, and these are effectively textured. This projection is developed considering information about the optical sensor architecture (internal parameters) and the platform position and bearing (external parameters). The collected multispectral data are usually transformed from Digital Numbers (DNs) values to both reflectance and several vegetation indices. Multispectral data along with the more traditional LiDAR height metrics are beneficial for predicting variables describing forest structural heterogeneity (Valbuena et al., 2018) and for improving public data through a building segmentation from Convolutional Neural Networks (CNNs) (Griffiths and Boehm, 2019).

In recent years, the proliferation of light-weight LiDAR sensors allows a physical integration of a multispectral camera and LiDAR sensor coupled to a UAV. In this way, simultaneous data can be acquired with a greater spatial resolution. Both sensors usually use the same GPS-IMU configuration to avoid the registration challenges caused by time–space inconsistency. Despite both sensors being mounted on the same platform, multispectral data must be calibrated following two main steps: (1) band-to-band multispectral image registration and (2) radiation correction model to solve the vignette effect. In this context, significant advances have been made focused on multi-sensorial data fusion. Sankey et al. (2021) proposed a novel methodology for UAV multispectral, hyperspectral and LiDAR data fusion in shrub-encroached desert grassland. However, this study is based on a comparison between 2D data using orthomosaics that are generated by Pix4D software (Pix4D SA, Lausanne, Switzerland), in the case of multispectral imagery, and SpectralView software (Headwall Photonics, Inc, Bolton, USA), to register the hyperspectral swatches. Gu et al. (2020) carried out a method to integrate UAV multispectral data and LiDAR models. This is based on an inner relationship between the multispectral grid pixel and the unorganized point cloud from the LiDAR sensor. To infer a model from 2D images to 3D physical world two components are considered: reflectance and shading.

The typical workflow of the proposed techniques involves the generation of a multispectral orthomosaic and then, an orthogonal projection is developed on 2.5D models. As shown in Fig. 5, orthomosaics are generated using either thermal, multispectral or hyperspectral images. However, the mosaicking process usually generates some misalignment areas derived from positioning errors. In addition, measured data are interpolated representing many viewpoints as one *ortho*-pixel. Despite recent advances fusing multispectral imagery and photogrammetric LiDAR point clouds, the preliminary results may be optimized in terms of computing time and spatial/radiometric resolution, since no real-time data fusion is mostly provided. Open lines are in progress using GPU devices as discussed in Section 4.4.

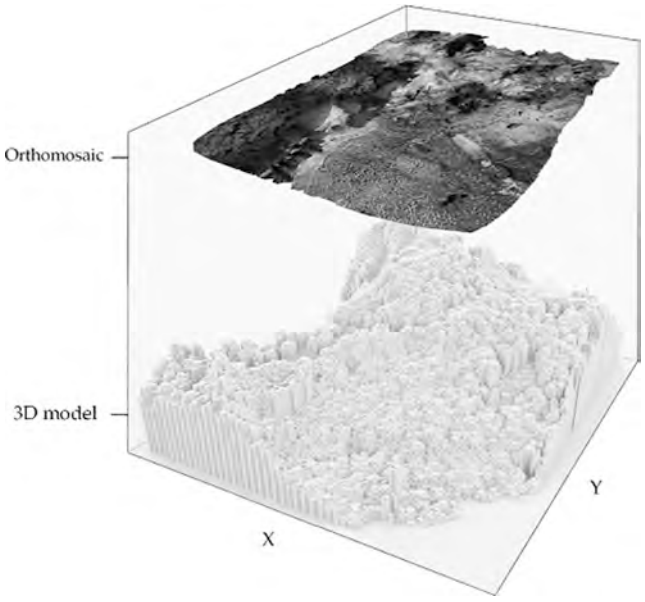

Fig. 5. Top-view projection of multispectral- thermal- or hyperspectral-orthomosaic into a 3D RGB point cloud represented as a 2.5D model through a voxelization.

4.2. Thermal imagery

Thermography or Infrared (IR) thermal imaging is a non-invasive technique that has rapidly evolved due to the enormous progress made in the last decades whether we consider the IR spatial resolution, noise levels, dynamic ranges, data storage capabilities and on-board image processing (Alfredo Osornio-Rios et al., 2019; Vollmer and Möllmann, 2017). Furthermore, competition in the industry of camera manufacturers has recently led to a significant drop in their prices, thus opening up a wide range of applications, both in research and industry fields (Vollmer and Möllmann, 2017).

4.2.1. Thermal overview

Visual cameras have been the standard imaging device, although their main acquisition challenges are their dependence on external energy sources, artificial or natural, to lighten the scene (Gade and Moeslund, 2014). Furthermore, they cover a small spectrum range, with wavelengths from 380 to 780 nm. Thus, thermal imaging arises as a passive sensing technology that provides additional information to detect and describe object surfaces at a temperature greater than absolute zero (-273 °C) (Gade and Moeslund, 2014; Tsouros et al., 2019; Vollmer and Möllmann, 2017).

IR imaging measures electromagnetic radiation emitted by surfaces in a small portion of the IR spectrum, ranging from 0.9 μm to 14 μm. Commercial cameras are available for three spectral ranges within the aforementioned range: short-wave (SW; 0.9 μm to 1.7 μm), mid-wave (MW; 3 μm to 5 μm) and long-wave (LW; 8 μm to 14 μm). In particular, thermal cameras commonly operate within the LW range (González et al., 2019; Vollmer and Möllmann, 2017) as it represents an atmospheric window and also contains the peak energy emission for most Earth surfaces (González et al., 2019; Quattrochi and Luvall, 1999).

Regarding their acquisition, aerial thermal imagery can be acquired from satellites and airborne platforms (Fig. 6), although their spatial and temporal resolution are commonly not adequate for monitoring tasks, not to mention their cost (González et al., 2019). For instance, China-Brazil Earth Resources Satellite (CBERS) observes the same area once every 16 days and presents a spatial resolution of 80 m per pixel ("INPE/CBERS," 2021), while Landsat operates with several platforms with a

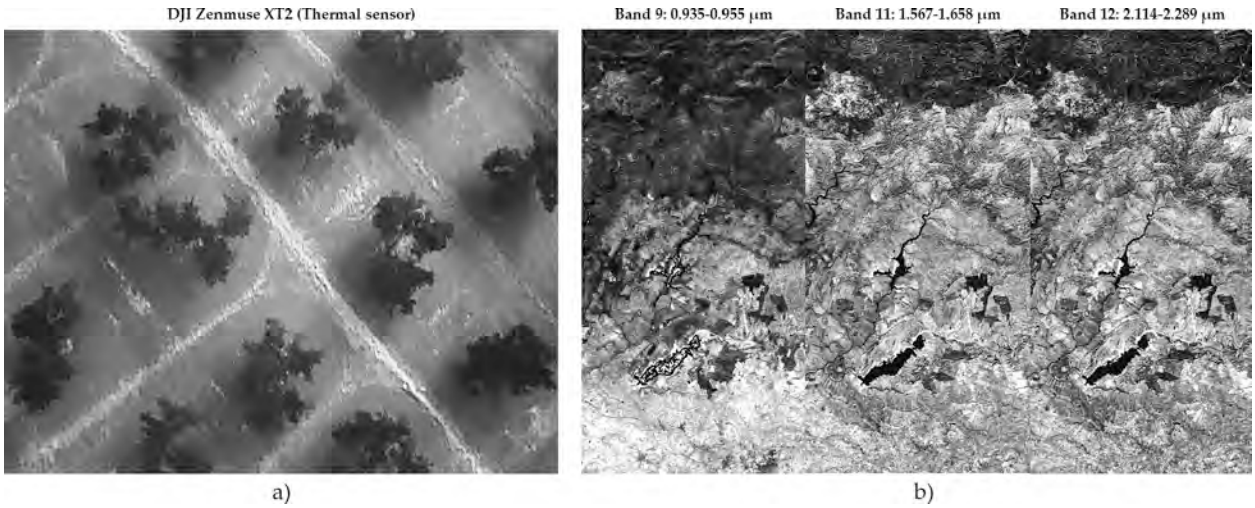

Fig. 6. Comparison of a) UAV-based thermal imagery with resolution 640x512 pixels and b) three satellite SWIR bands from Sentinel 2 mission within the Copernicus space program. The thermal sensor mounted on the UAV captures the spectral range 7.5–13.5 μm, whereas satellite bands present thinner intervals and cover mainly the SWIR wavelength range. Both images depict areas in the region of Jaén, Spain.

spatial resolution of 60 m and 100 m for Landsat 7 and Landsat 9, respectively, though it is typically resampled to 30 m (Landsat 9, n.d.). Therefore, UAVs emerge as an alternative to deploying low-cost and lightweight thermal sensors by operating as low-altitude satellites (González et al., 2019; Tsouros et al., 2019). Higher spatial and temporal resolution opens up fine-grain monitoring tasks, such as the management of geothermal features (Nishar et al., 2016), crop management, including the detection of plant diseases, (Yandun Narvaez et al., 2017; Zarco-Tejada et al., 2018) and error control in several industrial fields (Alfredo Osornio-Rios et al., 2019; McManus et al., 2016). Despite temperature has been described as an important parameter for crop monitoring activities, it usually requires multisensor approaches to increase the monitoring accuracy (Wachs et al., 2010; Yandun Narvaez et al., 2017). Hence, thermography can supplement other data sources for a better understanding of a particular environment (Hoegner et al., 2018, 2016b; Hou et al., 2021; Truong et al., 2017).

Consumer-grade thermal cameras are less expensive but also present lower resolution and defects. Among the available thermal sensors, Table 4 reports those sensors which have been previously used for research purposes. Though there exist hand-held devices, we have mainly described sensors that can be mounted on UAVs. Sledz et al. (2018) reported several sources of noise (environmental conditions, non-uniformity of Focal Plane Array (FPA), etc), causing thermal infrared (TIR) images to be commonly blurred and smoothed out (Javadnejad et al., 2020). As opposed to ideal optical imaging, the radiation of an object field is also observed by multiple neighboring detector elements (Vollmer and Möllmann, 2017). Beyond resolution challenges, the observation of thermal radiation is also error-prone for high-altitude platforms since it is attenuated by energy dispersion and atmospheric absorption (González et al., 2019; Quattrochi and Luvall, 1999; Vollmer and Möllmann, 2017). Though, this drawback is minimized using UAV platforms.

Although outdoor scenes are mainly surveyed through aerial platforms, it is also common to find research studies focused on terrestrial measurements and indoor environments. Terrestrial thermography is performed by means of several devices. Lin et al. and (2019b) and Stojcsics et al. (2018) collect thermal data from a hand-held camera, whereas Zhu et al. (2021) record both thermal and LiDAR from a multisensor vehicle. Adán et al. (2020) used a robotic platform to autonomously navigate and scan indoor environments. Previous work also exploited the use of custom systems that are geometrically calibrated by describing the lever-arm between multiple sensors (Hoegner et al., 2018; Javadnejad et al., 2020). This calibration is performed by collecting multiple images of a calibration pattern, either it is a common checkerboard (Javadnejad et al., 2020) or landmarks whose reflectivity facilitates their finding in thermal imagery (Adán et al., 2017).

Concerning TIR applications, they can significantly differ whether we consider their Infrared band. However, their overall applications include energy inspections on buildings and energy installations (Alfredo Osornio-Rios et al., 2019; Gade and Moeslund, 2014), detection of human and animal operators occluded by vegetation (Yandun

Table 4
Consumer-grade thermal devices that were explored in previous work. Their main characteristics are reported through their specifications, according to the manufacturer's source.

Device name	Focal length	FOV	Image resolution (px)	Spectral range	Research articles
DJI Zenmuse XT2	13 mm 19 mm	32°×26° 25°×19°	640 × 512 336 × 256	LW (7.5–13.5 μm)	(Jeong et al., 2021; López et al., 2021b; Yuan and Choi, 2021)
FLIR A320	18 mm	25°×18.8°	320 × 240	LW (7.5–13.5 μm)	(Guilbert et al., 2020)
FLIR A35	9 mm	48°×39°	320 × 256	LW (7.5–13.5 μm)	(Lorenzo Comba et al., 2019)
FLIR ONE	87.12 mm	50°×38°	80 × 60	LW (8–14 μm)	(Javadnejad et al., 2020)
FLIR A65	25 mm	25°×20°	640 × 512	LW (7.5–13.5 μm)	(Adán et al., 2017; Clarkson et al., 2017; Jarząbek-Rychard et al., 2020; Lin et al., 2019a; Westfeld et al., 2015)
FLIR Tau2 640	13 mm	45°×37°	640 × 512	LW (7.5–13.5 μm)	(Boesch, 2017; Sledz et al., 2018)
thermoMAP	N.A.	N.A.	640x512	LW (7.5–13.5 μm)	(Pádua et al., 2019)

Narvaez et al., 2017), as well as their tracking, biometric identification (Gade and Moeslund, 2014), detection of concerning biometric changes in animal production (McManus et al., 2016), an inspection of solar panels, structural assessment on industrial processes (Alfredo Osornio-Rios et al., 2019), etc.

Regarding crop and forest management, thermography is applied to tree characterization by measuring their energy flux, evapotranspiration and photosynthesis (Webster et al., 2018), as well as for water stress and disease detection (de Oca and Flores, 2021; Yandun Narvaez et al., 2017). Heating monitoring also prevents frost damage from crops (Yuan and Choi, 2021). Besides 2D analysis, the fusion of thermal data with 3D structures enriches environmental monitoring practices with 3D geometry. Therefore, it allows us to further evaluate the location of image details. In addition, 3D representations facilitate the embedding of thermal data in geodatabases (Antón and Amaro-Mellado, 2021; Lin et al., 2019a).

4.2.2. 3D reconstruction from thermal imagery

Although 3D structures involve both 3D point clouds and polygonal meshes, the first representation is the most conventional in the research field, whereas BIM (Building Information Modeling) models are also gaining interest as an accurate representation of real buildings for diagnostics and rehabilitation purposes (Hoegner et al., 2016a; Iwaszczuk and Stilla, 2017; Macher et al., 2019).

Despite this survey being focused on 3D modeling from remote sensing data and its application to forest and farming scenarios, most published studies related to thermographic 3D modeling explore their application in other fields, such as indoor and outdoor energy inspections in buildings. Furthermore, previous work concerning natural environments proposes naive approaches, as their main goal is to analyze vegetation features instead of the modeling procedure itself, as shown in Table 5. Thus, in this section, we aim to review 3D thermographic modeling techniques previously described in the literature, whether they are applied to fields of our interest or not. However, we also intend to discuss their applicability to forest and crop environments.

Despite the low resolution of thermal imagery, photogrammetric approaches such as SfM-MVS are commonly described to build thermal point clouds, as they are part of most commercial solutions for processing remote sensing information. Some notable software applications are Pix4DMapper (Zheng et al., 2020), Agisoft Metashape (Grechi et al., 2021; Guilbert et al., 2020; Lin et al., 2019a; Macher et al., 2019; Metcalf and Olsen, 2016), Autodesk Recap 360 (Lafi et al., 2017) or Zephyr (Clarkson et al., 2017; Maset et al., 2017), as they provide built-in 3D modeling tools based solely on photogrammetric techniques. Despite their simplicity, the reconstruction process becomes more challenging due to the aforementioned defects and limitations, which causes a significant reduction in the number of tie points during feature detection (Lin et al., 2019a). Consequently, resulting point clouds are sparser and less accurate whether we consider noise, gaps and incorrect spatial estimations, as reported in previous studies (Ham and Golparvar-Fard, 2013; Hoegner et al., 2016a; Kong et al., 2018). Beyond thermal imaging challenges, the reconstruction of 3D point clouds with SfM is also prone to errors for environments with repetitive patterns or uniform textures, e.g. buildings and vegetation (Jarząbek-Rychard et al., 2020; Lin et al., 2019a; Mathews and Jensen, 2013). Hence, photogrammetric approaches are expected to generate less accurate results in environments of our concern.

SfM has been extensively studied as a first step for 3D thermographic modeling (Clarkson et al., 2017; Dahaghin et al., 2021, 2019; González et al., 2019; Grechi et al., 2021; Guilbert et al., 2020; Hoegner et al., 2016b; Hoegner et al., 2016a; Hoegner and Stilla, 2018; Kniaz and Mizginov, 2018; Maset et al., 2017; Metcalf and Olsen, 2016; Nishar et al., 2016; Sledz et al., 2018; Webster et al., 2018; Westfeld et al., 2015; Zheng et al., 2020). However, the resulting point clouds typically suffer from insufficient resolution for monitoring tasks. Additionally, the recognition and marking of GCPs to accurately align the point cloud in a global coordinate system is limited in thermal imaging due to their low spatial resolution and contrast (Sledz et al., 2018). Consequently, SfM is frequently followed by several refining operations, mainly by using other data sources that provide the missing accuracy. Nevertheless, previous research has explored the reconstruction through SfM and the conventional marking of GCPs as the unique stage to further explore some of the cited applications (Dahaghin et al., 2021, 2021; González et al., 2019; Metcalf and Olsen, 2016; Nishar et al., 2016; Sledz et al., 2018; Zheng et al., 2020). To solve the limited visibility of GCPs in thermal imagery, Boesch et al. (2017) and Nishar et al. (2016) used metal-coated GCPs with low emissivity in comparison with the surrounding vegetation. An example of non-metal coated GCPs is shown in Fig. 7. Previous work has also assessed the enhancement of the accuracy of External Orientation Parameters (EOP) by replacing the EOP estimated from devices with higher precision (e.g., RGB devices) (Jeong et al., 2021).

Additionally, some preprocessing methods have been proposed to optimize photogrammetric procedures. Maes et al. (2017) estimated the parameters of the thermal camera using the Brown-Conrady distortion model. They proposed to correct temperature by decoupling the influence of air temperature throughout several flights and improvements in image position were achieved considering the on-board GPS/GNSS log file.

Table 5
Classification of methods for 3D thermal modeling related to forestry and agriculture, according to the preprocessing of thermal images (Thermal data source) and their registration to a global coordinate system (Registration). Alternative 3D models are mainly provided by reconstructed RGB and LiDAR point clouds.

Thermal data source	Registration	Previous work
Thermal point cloud	Ground Control Points (GCPs)	(Boesch, 2017; González et al., 2019; Guilbert et al., 2020; Nishar et al., 2016)
	GCPs and ICP with an alternative 3D model	(Webster et al., 2018)
Thermal orthomosaic	Alternative 3D model	(Lorenzo Comba et al., 2019; Neale et al., 2011a)
Thermal images	Alternative 3D model	(Hosoi et al., 2019; López et al., 2021b)

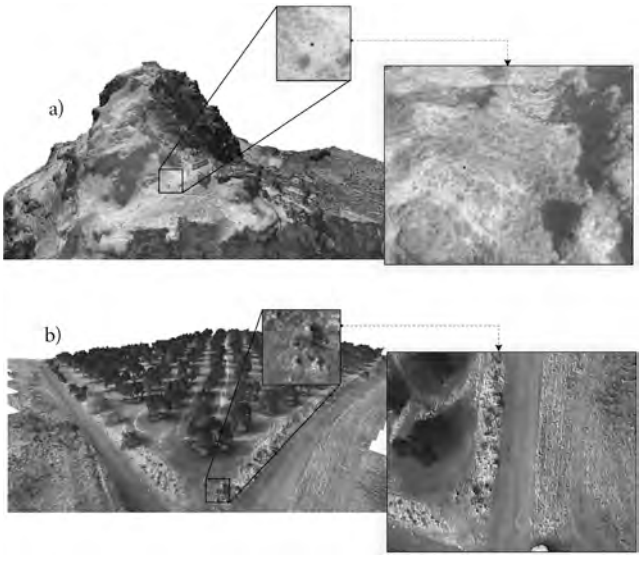

Fig. 7. Non-metal coated GCPs and their representation surrounded by different materials. As depicted, GCPs cannot be properly marked over some environments (b) whether the neighboring materials present similar radiance behavior.

To overcome the limitations imposed by SfM keypoint detection, several studies propose alternative algorithms to enhance both feature extraction and the discard of false matching of point pairs. In this regard, Kong et al. (2018) discarded mismatches by applying first a K-Nearest Neighbor algorithm (KNN) to remove obvious false matches, followed by a modification of AC-RANSAC that includes the temperature as a constraint to distinguish correct matches from mismatches. As opposed to the RANSAC algorithm, both procedures are not dependent on a threshold given by model hyperparameters. On the other hand, feature descriptors are altered whether thermal imagery is merged with other data sources, e.g. RGB high-resolution imagery.

4.2.3. 3D reconstruction from multi-source imagery

Rather than building solely a 3D thermal model, the fusion of several data sources has been extensively investigated. RGB images are the main data source for 3D reconstruction, as they present higher resolution and thus allow producing more accurately dense 3D models. Therefore, most of the previous work is based on the building of RGB point clouds and the subsequent projection/alignment of thermographic information (Hosoi et al., 2019). Registration of visible and thermal imagery is performed through feature descriptors, either they are in 2D or 3D. Consequently, keypoints visible on both spectral ranges are automatically matched and filtered out to discard mismatches. Hence, the matching of features allows correlating both multidimensional data sources and projecting 3D RGB points into thermal imagery. Therefore, methods based on the projection yield large point clouds with upsampled thermal information.

Some methods found in the literature consider that visible and thermal imagery can be perfectly aligned without any further registration processing (Hou et al., 2021; Stojcsics et al., 2018). Under normal conditions, visible and thermal images are rarely corresponding to a fixed area due to device calibration, the delay between captures and vehicle movement (López et al., 2021a). This is valid, even for co-acquired images. As a result, image registration is refined by finding an affine or homography matrix to handle minor misalignments for co-acquired images. Unordered images are commonly handled by fusing 3D and 2D models. Other alternatives to avoid the alignment of images using their color data are based on the calibration of a multisensory system. Thermographic sensors are frequently combined with RGB cameras (Adán et al., 2017; Dino et al., 2020; Hoegner et al., 2018; Javadnejad et al., 2020; Landmann et al., 2019) and LiDAR sensors (Adán et al., 2017; Hoegner et al., 2018). To calibrate a dual-sensor co-registration, previous work estimated translation (lever-arm) and rotation (boresight) matrices to represent the relative difference between both systems through semi-automatic and manual identification of intensity features visible on any pair of images. Although this approach is theoretically correct, methods based on image registration that do not rely on *a priori* geometric calibration are proved to perform better in consumer-grade thermal cameras (Javadnejad et al., 2020). Once the relative transformation is known, either in 2D or in a dual-head system, RGB points can be projected into thermal imagery. Finally, larger point clouds can also be generated by mixing both RGB and thermal imagery in the bundle adjustment phase of SfM, followed by the generation of a dense point cloud that only integrates RGB data. As a result, thermographic information is described with respect to RGB by means of SIFT features and the point cloud can be subsequently projected into thermal images (Hoegner et al., 2016b). However, it relies on SIFT capabilities for detecting features on images with different radiometric behavior.

Regarding methods for image registration, as shown in Table 6, the main challenges concern the feature descriptor used to detect features, as edge detectors typically replace conventional descriptors, such as SIFT or SURF. For that purpose, Canny and Sobel filters have been previously applied to contour detection, thus allowing to obtain an affine transformation to register similar images (Bennis et al., 2013; Hoegner et al., 2016a, 2016b). The resulting contours can also be filtered out to extract only prominent edges through Hough transform

Table 6
Summary of previous work concerning feature matching to estimate camera poses and reconstruct 3D models, either in 2D, 3D or both domains.

Domain		Algorithm		Previous work
RGB	Thermal	RGB	Thermal	
2D		ECC		(López et al., 2021b)
		SIFT		(Hoegner et al., 2016a, 2016b)
		RIFT		(Lin et al., 2019a)
2D		Sobel		(Hoegner et al., 2016a, 2016b)
3D	2D	Delaunay	Canny	(Bennis et al., 2013)
		Harris		(Zhu et al., 2021, 2019)
		Plane estimation	Sobel + Hough	(Hoegner et al., 2016b)

(Hoegner et al., 2016b). These solutions are adopted to overcome SIFT limitations whether we use imagery with non-linear gradients. Nevertheless, they can be hardly applied to natural environments with significant vegetation density since edges are not relevant enough for their pairing (Fig. 8). López et al. (2021b) solved the registration of visible and thermal imagery showing natural environments through an optimization technique called Enhanced Correlation Coefficient (ECC), based on the finding of the transformation matrix that maximizes the correlation coefficient. Given the limitations of linear-gradient feature extraction, previous work also describes methods based on the frequency domain to handle nonlinear radiation differences in thermographic and visible images, such as Radiance Invariant Feature Transform (RIFT) (Lin et al., 2019a). Feature matching methods can be

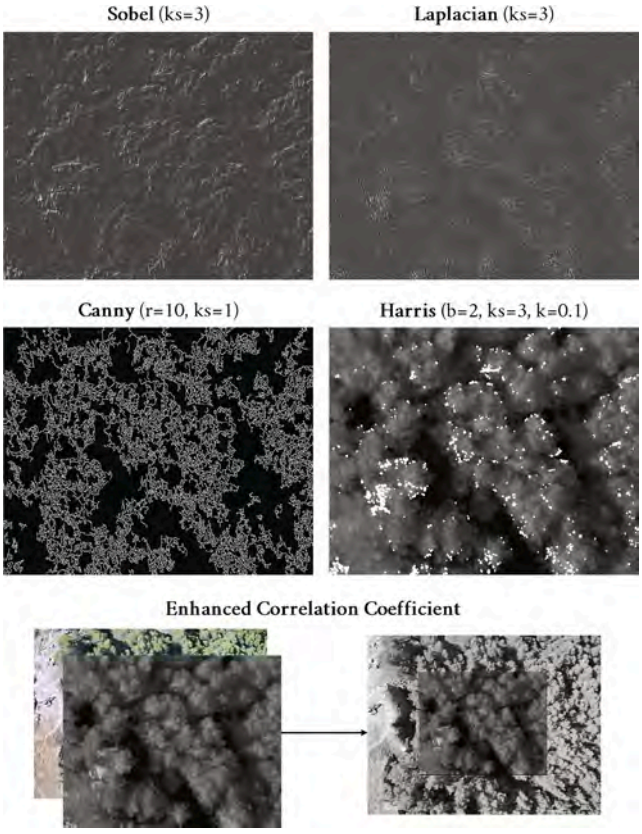

Fig. 8. Comparison of the core of several registration algorithms. Edge-based descriptors are shown as insufficient methods for environments with dense vegetation, while methods not dependent on a linear gradient, such as ECC, are proved to perform better. *ks* refers to kernel size, the ratio is presented as *r*, and *k* is a free parameter on the Harris detector. The brightness of the two first images is increased to improve the visualization.

followed by techniques to discard mismatches, such as RANSAC (Lin et al., 2019a). Once images are registered, whether the projection of RGB captures is known, 3D points are projected into thermal images.

Supervised procedures are also possible by manually selecting the corresponding pairs of RGB and thermal points. Ham and Golparvar-Fard (2013) estimated the Epipolar geometry between both camera systems by manually picking image features, whereas (Huang et al., 2018; Macher et al., 2019) supported their decision through checkerboard images and relevant image key-points, e.g. building corners. Lafi et al. (2017) performed semi-automatic stitching of thermal images by marking relevant features on thermal images, thus generating a panoramic image to be mapped to a 3D RGB point cloud. However, methods based on semi-automatic registration are not appropriate for datasets composed of a considerable number of images. In fact, their main advantage is the generation of thermographic models using a few images, instead of larger datasets.

Projection can also be performed by mixing both 3D dense point clouds and thermal imagery. For that purpose, the Perspective n Point (PnP) optimization problem is solved by pairing 3D and 2D features, thus estimating the camera pose. As previously described, they typically extract edge features. Although SIFT descriptor may be used in 2D, 3D and 2D must find similar features, whereas SIFT3D is reported to identify an insufficient number of keypoints. Hence, contours-based approaches replace conventional SIFT descriptor through Harris and Harris3D operators (Zhu et al., 2021, 2019). Moreover, Harris3D is shown as a robust method whose detected features are less likely to appear in other location in a single image. Instead of considering contours as significant features, Lin et al. (2019b) proposed to use the line intersections as key points. Nevertheless, there is seldom a robust method to accurately match 2D and 3D features. Therefore, the pairing is mainly performed by a human operator (Zhu et al., 2021, 2019) or by restricting the search space through GPS/GNSS data, along with RANSAC to discard mismatches (Lin et al., 2019a). Consequently, other approaches seem to be more adequate and applicable to forest and agriculture applications, although using a reduced search space and extracting features concerning several edges (e.g., intersections) may increase its degree of applicability.

The reconstruction of accurate RGB point clouds is also tempting for naive approaches based on the registration of both point clouds, in spite of the density and noise gap. This approach is suitable for reconstructions of thermographic models with sufficient density and quality. Therefore, alignment procedures benefit from RGB fine registration to obtain a multi-source environment that enhances the positioning of thermal models. Consequently, monitoring tasks perform further processing with RGB and thermal data. Minimization of differences between two point clouds can be performed through Iterative Closest Point (ICP) by estimating the composite matrix of translation and rotation (scaling may also be considered) (Clarkson et al., 2017; Hoegner et al., 2016b; Hoegner and Stilla, 2018; Lin et al., 2019a; Maset et al., 2017; Webster et al., 2018; Westfeld et al., 2015). Webster et al. (2018) surveyed canopies through a LiDAR sensor instead of visible imagery. Rather than apply the raw ICP algorithm, thermal point clouds can be preprocessed by applying noise filtering and a coarse global registration through a rigid body transformation using the camera poses (Truong et al., 2017), whereas the ICP algorithm constitutes a local registration. An alternative to ICP is Fast Global Registration (FGR), which is proven to achieve better results for noisy datasets (Lin et al., 2019a). Point clouds can also be registered by means of at least three GCPs whether they can be accurately identified on thermographic reconstructions (Dahaghin et al., 2019). In addition, the use of ICP along with KNN has been investigated to assign thermal data to RGB points, whose output is a dense 3D model with upsampled thermal information. Instead of performing this fusion in 3D space, more accurate results are achieved by projecting images directly into a dense visible point cloud.

Building thermographic 3D models can also be performed by combining 3D point clouds generated by device alternatives to thermographic tools, such as LiDAR or visible sensors, with thermal maps placed in a common coordinate system. Comba et al. (2019) and Neale et al. (2011b) fused RGB point clouds with a registered thermal orthomosaic, whereas Adán et al. (2020) combined LiDAR results with 360-degree maps of thermographic information. Hence, this approach relies on the generation of a thermal composition of limited resolution and its subsequent projection to a 3D model. In fact, these methods approximate a 2.5D model by providing depth values to thermal information (Juszczyk et al., 2021). Therefore, their results are more likely to present occluded areas that cannot be analyzed. Adán et al. (2020) overcame this challenge through a mobile scanning platform and the fusion of several thermal point clouds retrieved from different viewpoints by using the platform odometry and the ICP algorithm.

4.2.4. Occlusion on 3D thermal reconstruction

The projection of 3D points into thermal imagery poses challenges in terms of occlusion and sample aggregation. Firstly, occluded points may receive thermal information from foreground objects since their projection in thermal imagery may be feasible and output valid coordinates within the image space (Fig. 9). On the other hand, a 3D point is more likely to be visible from multiple images, thus receiving distinct thermal samples (López et al., 2021b). The occlusion of 3D point clouds is frequently omitted due to their discrete representation, whereas polygonal meshes are easier to operate. However, the reconstruction of a mesh from a point cloud is not trivial for vegetation. Moreover, methods described in the literature for the estimation of a triangle mesh are dependent on several parameters to be adapted for each individual scenario (Cohen-Steiner and Da, 2004). Occlusion is mainly handled by using the well-known z-buffer (or depth buffer), where pixels of every image are mapped to one 3D point at most, i.e., the nearest point to the image viewpoint (Jeong et al., 2021; López et al., 2021c, 2021b). This method can also be adapted to sub-pixel SfM approaches since the dimensions of the depth buffer determine its level of detail. López et al. (2021b) also managed the occlusion through a 3D approach, where points are represented by a spherical volume whose size depends on their distance to the image viewpoint, considering the GSD. Nevertheless, 3D techniques require building data structures to accelerate queries on ray-volume intersections, such as the Bounding Volume Hierarchy (BVH) (Meister and Bittner, 2018). Remark that these data structures need to be built for each image, using a point subset consisting of several millions of volumes.

Regarding aggregation of multiple samples, previous studies have conventionally averaged them (Hoegner et al., 2016b; Javadnejad et al., 2020). Whether we consider individual samples to be consistent enough by themselves, maximum, minimum and any other averaging functions are presented as valid operators (Jeong et al., 2021). However, the selection of a suitable operator may be based on visualization results or

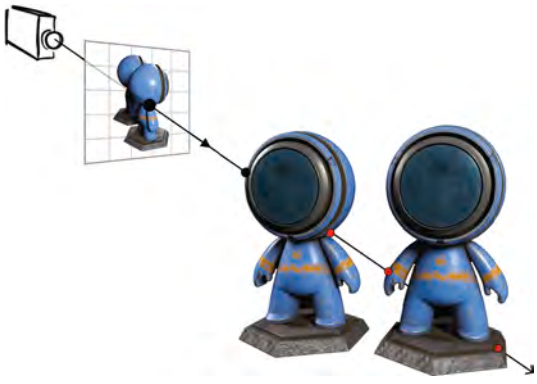

Fig. 9. Representation of an occlusion scenario, where multiple 3D vertices along a ray are projected within the image plane. Though, the right model is occluded by the first figure.

metrics measuring the distance of the aggregated results from image samples (López et al., 2021b). Whether we aim to reduce distance with respect to original thermographic information, a penalty function is proposed to measure the error between the aggregation and multiple image samples, thus allowing to generate a recognizable compressed model as shown in Fig. 10.

4.2.5. Temperature extraction

Resulting point clouds from previous methods are regarded as grayscale intensity values, whereas thermal imagery provides further data as absolute temperature values. Accurate radiometric calibration has been previously encountered and handled through different methods (Fig. 11).

Some devices allow capturing images in specific radiometric file formats containing several embedded parameters that enable the reconstruction of temperature values by applying the formula given by the manufacturer (López et al., 2021b; Teza and Pesci, 2019; Westfeld et al., 2015). For instance, FLIR One and Zenmuse XT2 allow recording RJPG imagery. The main advantages of radiometric file formats are their flexibility to modify emissivity factors from surfaces in the given formula. However, other file formats provide a digital number of *n*-bits which represents the output of the formula, thus presenting lower adaptability. Their translation to absolute temperature relies mainly on device functioning, as high/low resolution are assigned different factors (Zheng et al., 2020) in a linear equation as the one shown in Eq. (1):

$$T_{abs} = F^{*}DN - 273.15 \quad (1)$$

where 273.15 is the conversion factor between Kelvin and degrees, and F represents the previous factor related to devise resolution.

Eq. (1) can be reformulated whether DN is given by a function fitting grayscale values and digital numbers (Zheng et al., 2020). Linear interpolation is also approached by integrating maximum and minimum temperature within the surveyed environment (Antón and Amaro-Mellado, 2021; Javadnejad et al., 2020). Finally, there exist commercial solutions to output temperature information from images, e.g., FLIR ResearchIR (Metcalf and Olsen, 2016).

4.3. Hyperspectral data

Following the latest developments both in unmanned aerial vehicles (UAVs) and in their associated technologies, new sensors have emerged.

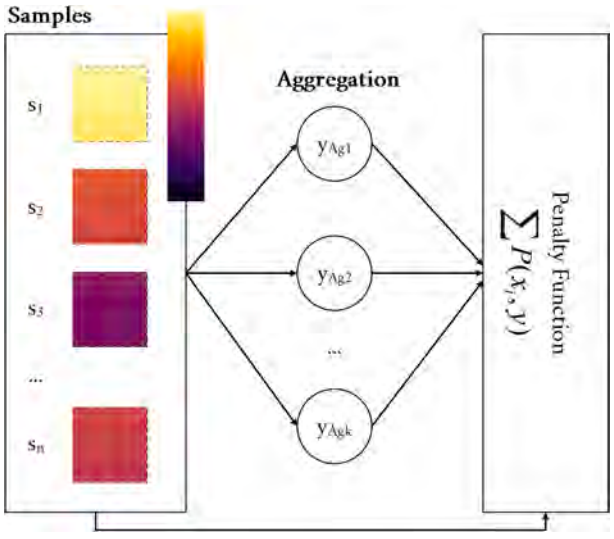

Fig. 10. Overview of a penalty function that receives as input the original thermal measurements as well as the values aggregated by different operators, in order to measure the error from samples to the aggregation.

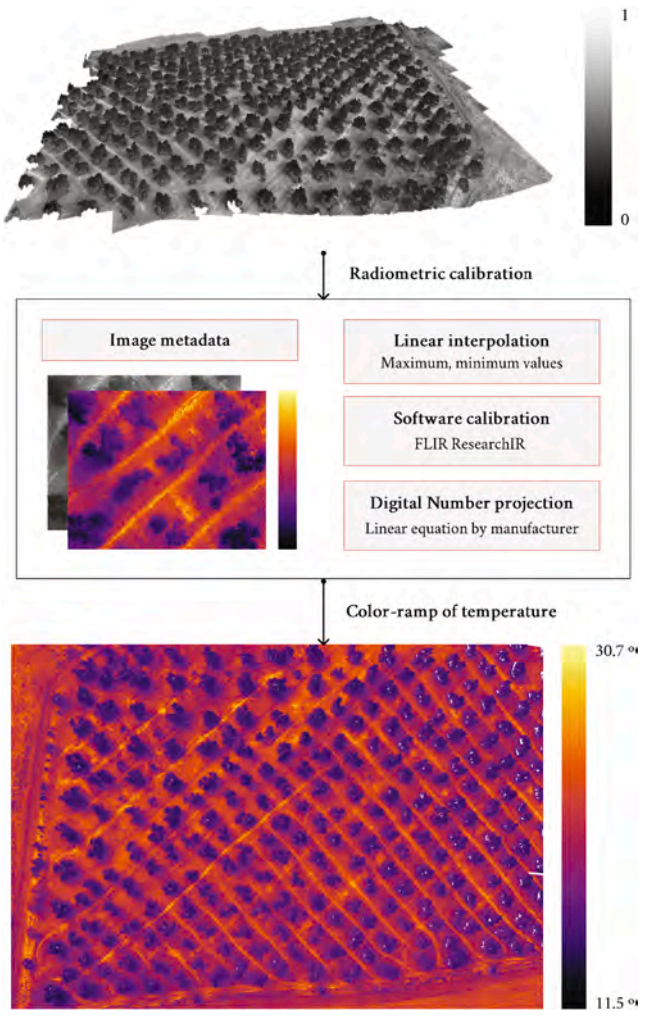

Fig. 11. Scheme of a radiometric calibration procedure. Different methods are depicted here to extract the temperature of a thermal image.

The more conventional and affordable sensors, presented in the previous sections, towards the integration with 3D data, have proven their usefulness in many applications. When spectral resolution is not a requirement, significant outputs for the interpretation and understanding of the phenomenon under study are derived. However, in some applications, there is a need to explore in greater detail the electromagnetic spectrum. In those cases, the accuracy and the spectral range of the conventional sensors may not suffice. In fact, for specific purposes, there may be a need to measure in detail several regions of the electromagnetic spectrum. To this end, it is explored the fact that objects' reflectance properties depend on the material and its physical and chemical state, as well as the surface roughness and sunlight incidence angle (Lombardo et al., 2020). The sensors that allow recording hundreds of spectral bands are called hyperspectral sensors and were initially employed in satellites and manned aircrafts. UAVs equipped with hyperspectral sensors provide new options to study high-resolution multi-temporal spectral data. A list of them is shown in Table 7.

For each pixel in an image, a hyperspectral sensor acquires the light intensity (radiance) for a large number (typically a few tens to several hundred) of contiguous spectral bands. Every pixel in the image thus contains a continuous spectrum and can be used to characterize the objects in the scene with great precision and detail. Therefore, hyperspectral sensors sample the spectral irradiance of a scene and collect three-dimensional (3D) data: two dimensions (x, y) representing the spatial coverage and the third dimension showing the spectral information (λ), originating from the so-called datacube. Thus, each pixel is

Table 7
List of some hyperspectral sensors used for UAV-based HSI acquisition and its main characteristics.

Manuf.	Sensor	No. of spectral bands	Spectral range (nm)	Acquisition type	Weight (gr)	Research articles
Headwall Photonics	Nano HyperSpec	272	400–1000	Push-broom	1200	(Li et al., 2017; Sankey et al., 2017, 2018)
Cubert GmbH	UHD 185 Firefly	138	450–950	Snapshot	490	(Aasen et al., 2015; Cao et al., 2018; Yue et al., 2018)
Senop	HSC-2 hyperspectral camera	Up to 1000	500–900	Snapshot	990	(Chan et al., 2021)

formed by a specific spectral profile containing location data, followed by hundreds of digital numbers aligned with the corresponding spectral bands.

Typically, four approaches can be used for acquiring hyperspectral imagery (HSI) in remote sensing. However, most sensors used in UAVs are classified as push-broom or snapshot. Since datacubes have a higher dimensionality than the two-dimensional (2-D) detector arrays currently used in RGB and multispectral sensors, system designers must resort to either measuring time-sequential 2-D slices of the cube (push-broom) or simultaneously measuring all elements of the datacube by dividing it into multiple 2-D elements that can be recombined into a cube in post-processing. Fig. 12 illustrates the main principles behind push-broom and snapshot approaches.

Push-broom sensors include an input aperture (a long slit). A set of 2-D detectors is used, so that all points along the line represented by the slit are sampled simultaneously. To form the complete 2D image of the area of interest, the sensor is moved in the direction orthogonal to the slit. In the specific case of this review, the UAV that carries the sensor plays this role. The array of detectors is pushed along the flight direction to scan the successive lines, and hence the name push-broom. Instead of a line scanner, the snapshot approach allows simultaneous recording of spatial and spectral information. This type of sensor enables the acquisition of a complete spectral data cube in a single integration, generating images from the areas of interest. This approach allows to directly acquire data, which reduces the post-processing complexity to obtain a 3D data cube.

It is worth noting that the type of sensor greatly affects field operations, processing performance and the quality of the final product. More information regarding hyperspectral technology can be found in Adão et al. (2017). UAV-based hyperspectral technology continues to be developed. The fact that it allows us to obtain information in hundreds of adjacent narrow bands, will enable the acquisition of more complete information about the imaging scene, material or phenomenon. The fusion of different types of data with 3D information, regarding agricultural and forest applications, is the focus of this review. Considering hyperspectral data and 3D information fusion, it would provide a more accurate scene understanding. This would also allow the development of unsupervised automatic sampling of meaningful material classes from the target area exploring new machine learning approaches.

Methods to compute 3D hyperspectral models were proposed in close-range applications. For instance, Zia et al. (2015) developed a method that applies structure from motion to images from different wavelengths and a 3D registration method to combine band-level models into a single 3D model. Yet, this method was applied neither in vegetation nor remote sensing HSI, only to objects in a controlled environment, by capturing images at different bands in the same position. Behmann et al. (2015) proposed a method to generate 3D models from push-broom HSI with potential for crop plant phenotyping in close-range applications. The method uses a polynomial image transformation to describe the non-linear effects occurring in plant phenotyping, considering not only the linear model of the push-broom sensors but also other distortion factors. Such 3D models were used to detect disease symptoms (Roscher et al., 2016) and data fusion with laser scanner models were also addressed (Behmann et al., 2016).

However, methods that are applied in laboratory conditions benefit from a controlled environment and sensor orientation stability, which is challenging to ensure in a natural environment for remote sensing applications, since that orientation conditions are always changing not only due to the orientation of the acquisition platform itself but also due to possible wind influence causing vibration to be induced on the sensor and in changes in the monitored scenes (Kalisperakis et al., 2015). Other works were capable of merging hyperspectral data in 3D models

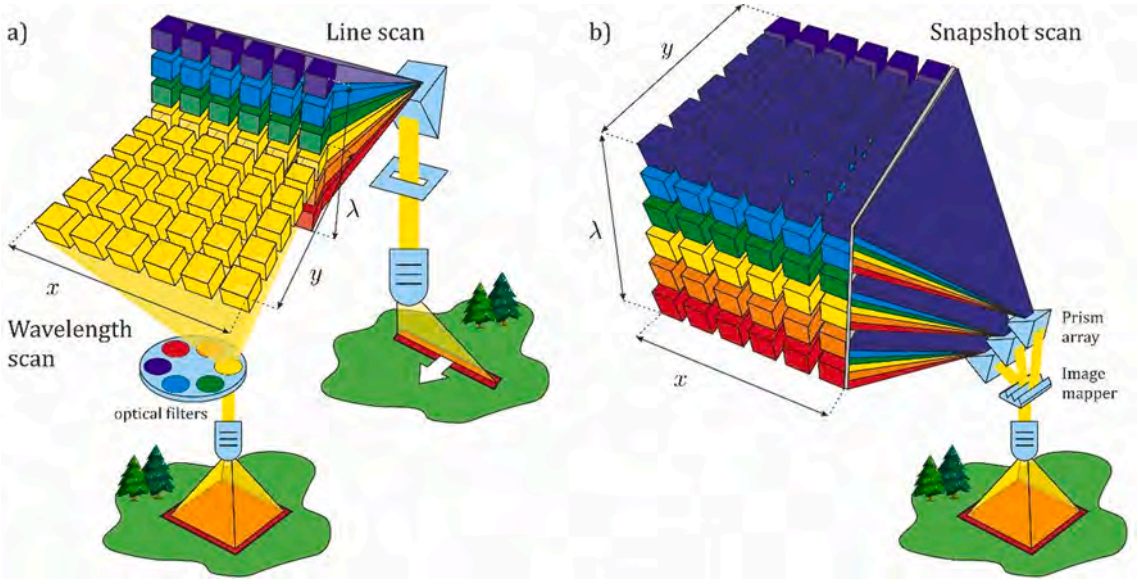

Fig. 12. Portions of the data cube collected for a single detector integration period for (a) push-broom and (b) snapshot devices.

generated from standard RGB cameras or laser scanning, which enabled the 3D geological modeling (Nieto et al., 2010) or 3D mapping of underwater environments (Ferrera et al., 2021). Liu et al. (2020) provided an in-depth review of HSI and 3D technologies for plant phenotyping by analyzing the literature from close-range applications to remote sensing.

In what concerns UAV-based remote sensing, the main focus of this paper, despite the flexibility offered by small-sized unmanned aerial systems, which enable data acquisition with high spatiotemporal resolutions than other remote sensing platforms (Pádua et al., 2017), the integration of hyperspectral sensors in UAVs is restricted due to payload capacity and flight autonomy (Adão et al., 2017; Bruning et al., 2020). These facts limit their employment to the monitoring of small-scale areas and research-oriented applications. Even so, UAV-based 3D hyperspectral is a recent and powerful technology that has become available to small-sized UAVs during the last decade (Nevalainen et al., 2017). Some approaches use non-imager spectrometers in UAV platforms along with an RGB sensor to accurately display the acquired spectral signatures on the 3D information generated from photogrammetric point clouds and orthophoto mosaics (Garzonio et al., 2017). Astor et al. (2020) combined UAV-based RGB data with ground-based snapshot HSI for biomass estimation in different vegetable crops. In what concerns the use of HSI in forestry and agriculture there are several approaches in literature exploring this topic. In the specific case of forestry studies and other ecosystems, in the vast majority, hyperspectral data acquired from different types of sensors is mainly used for species classification and estimation of structural parameters.

Regarding 3D data fusion of HSI, the challenges arise due to both data dimensionality and therefore storage capacity, more specifically, due to the nature of its data acquisition process. If HSI is acquired by using a snapshot sensor, a 3D context can be easily obtained since this data can pass through a photogrammetric processing pipeline. However, if a push-broom sensor is used instead, the challenges are complex to solve, since this data is generally computed in a raster form with optimal results for each swath. In the studies addressing this topic, LiDAR data was used for data fusion (Lin et al., 2019b; Sankey et al., 2017, 2018), nevertheless, the data fusion can benefit from work developed in the integration of these sensors in airborne platforms for vegetation monitoring (Mitchell et al., 2015; Torabzadeh et al., 2014). If multiple swaths are intended to be merged, there can be issues with stitching them together. Several approaches were already proposed concerning this issue by performing co-registration based on feature detection on RGB and HSI imagery (Angel et al., 2020; Fang et al., 2019; Jurado et al., 2021) which can help in combining push-broom HSI with 3D photogrammetric point clouds.

Nevertheless, since the data is acquired by scanning, few perspectives of the surveyed area are acquired (only in the direction of the flight lines), thus making a full 3D data acquisition from complex objects, which are the case of trees and crops. Methods that account for this spatial heterogeneity to correctly merge hyperspectral data from push-broom sensors into the 3D space are lacking in the literature. With such approaches, it would be possible to have a seamless data fusion integration that allows a very high spatial and spectral data availability, opening alternatives to study different scenarios by visualizing spectral signatures in different parts of the area under study. It can be expected that in the near future UAV-based hyperspectral sensors would be capable of acquiring data in other parts of the electromagnetic spectrum as short-wave infrared to extend capabilities of aerial spectroscopy in vegetation monitoring or even HSI on-board real-time data processing, in fact some proposals were already presented towards this direction (Horstrand et al., 2019; Saari et al., 2017).

4.4. GPU-based acceleration for data computation

The increase of data volume in terms of quantity and spatial resolution involves high-computational efforts for image stitching, matching and processing. Moreover, multi-source data integration and operations with large and dense 3D models can be sped up using parallel computing, although these algorithms are mainly constrained by the limited GPU memory (up to a few GBs). Nowadays, popular commercial solutions benefit from CUDA-compatible GPUs. For instance, Pix4D-Mapper and Agisoft Metashape enable the execution of photogrammetric procedures in GPU. Despite their hardware acceleration, most of them present a significant response time whether datasets consist of several hundreds of images, both for feature extraction and the building of a dense point cloud (Lafi et al., 2017). Whether we consider common commercial software already includes GPU computing, the exploration of alternative 3D modeling techniques is also studied in GPU, mainly for complementary data sources. For instance, the projection and occlusion in multispectral 3D point clouds is solved in GPU for point clouds of up to 271 million points and 1352 images (López et al., 2021c).

Beyond the SfM procedure itself, post-processing techniques concerning 3D models are also well suited for their parallel development. Whether we aim to project new data sources into 3D models, we need to consider the occlusion to assign additional values to foreground objects. Hence, the occlusion detection requires iterating over the complete image dataset if solved in 2D. Consequently, its implementation is highly parallelizable, as shown in (López et al., 2021c, 2021b), thus requiring a few seconds to solve the occlusion problem, instead of requiring several hours. Normal estimation is also well suited for its development as a massively parallel methodology, as each point can find its surrounding points and estimate the normal vector (Jurado et al., 2020a; López et al., 2021b). Given the nature of the revised data sources, specific scenarios may require transmitting information from remote locations and over low-bandwidth networks. Hence, their compression is a key factor for real-time monitoring. Additionally, compression algorithms are time-consuming tasks, thus High-Performance Computing (HPC) and hardware accelerators field-programmable gate arrays, such as FPGA, are frequently utilized to speed-up compression methodologies (Dua et al., 2020). Remark that compression affects single hyperspectral captures as well as multi-temporal datasets.

5. Discussion

The integration of multispectral data and 3D models involves many recent solutions to monitor and study both morphological and physiological traits. The combination of spectral bands enables the calculation of different radiometric indices (NDVI and NDWI) and with the addition of LiDAR-derived DEM layers, Yeo et al. (2020) developed a method for vegetation classification and mapping of saltmarsh habitats. Previous work fused LiDAR data and multispectral imagery for disease detection, biomass estimation, crop monitoring, forest inventory, etc.

The spatial resolution of LiDAR data is increasing so that the integration of such 3D models with UAV-multispectral images leads to develop deep learning methods for the classification of tree species (Briechle et al., 2020), recognition of invasive species (Dash et al., 2019) and early detection of tree diseases (Yu et al., 2021). Other studies were proposed for the generation of multispectral 3D models by mapping multispectral images on dense RGB point clouds (Jurado et al., 2020b), the extraction of 3D individual tree structure (Dai et al., 2018) and the semantic segmentation of 3D models (Jurado et al., 2020a), lastly using deep learning approaches (Jing et al., 2021). The generation of multispectral 3D data presents many advantages for multiple applications since apart from the color, other spectral values can be studied and represented. Fig. 13 illustrates a general overview of preliminary results of existing methods for the reconstruction of 3D thermal and multispectral point cloud using UAV imagery.

Due to its early state in the RS field, thermal data acquired in forestry environments has been mainly applied on multi-source fusion algorithms, thus addressing their applicability to scenes that pose a challenge for photogrammetry (Boesch, 2017; Guilbert et al., 2020; López et al., 2021b; Nishar et al., 2016). Regarding 3D thermal research, previous studies describe the monitoring of radiation inertia (dynamics)

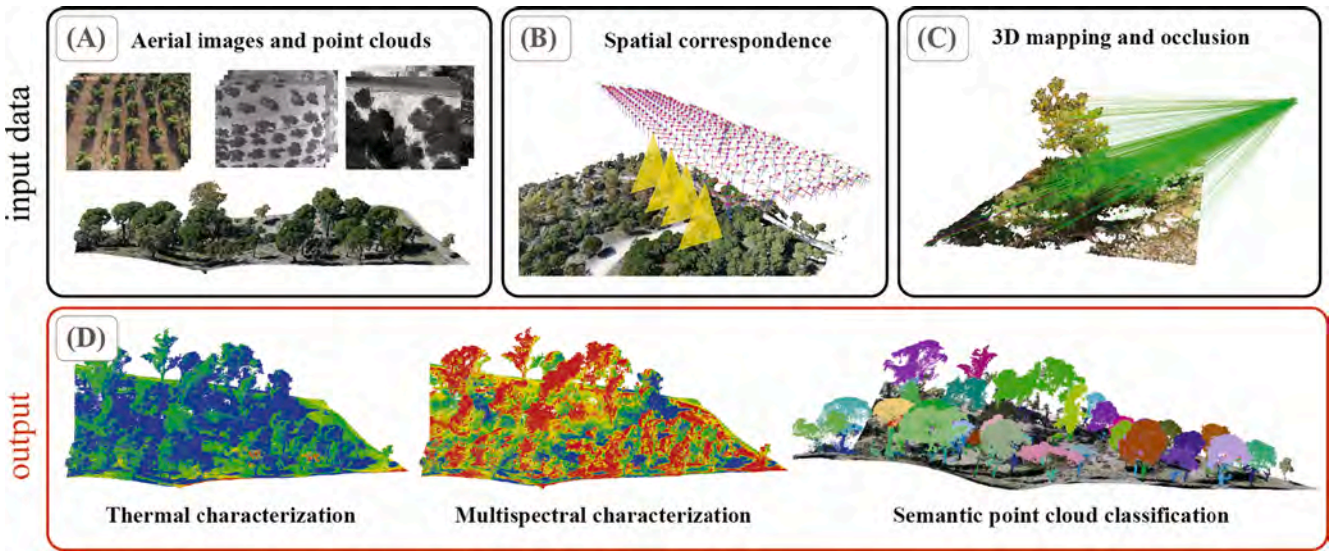

Fig 13. Illustration of the point cloud characterization by 3D mapping of multi-source UAV images. Panel (A): a 3D point cloud and datasets of aerial images are shown with high-resolution RGB, thermal and multispectral images. Panel (B): a spatial correlation is defined to set the point clouds and all cameras in the same reference system. In Panel (C): the processes for image mapping on the 3D geometry and occlusion tests are depicted. Panel (D): several outputs and applications through the fusion of multi-sensor imagery and 3D models. The first figure shows a thermal distribution on the point cloud (López et al., 2021b), the second figure is obtained by the spectral image mapping on the point cloud (Jurado, 2020) and the last one shows the semantic segmentation of the 3D model considering all previous attributes assigned per each 3D point (Jurado et al., 2020c; Mäyrä et al., 2021).

on crop soils (González et al., 2019), the temperature of forests with regard to the canopy height (Webster et al., 2018), crop classification considering their vigor (Lorenzo Comba et al., 2019), estimation of evapotranspiration and water, allowing to classify species (Neale et al., 2011a) and chlorophyll estimation (Hosoi et al., 2019). Hence, overall 3D thermographic research aims to provide long-term monitoring of crops and forestry, thus enabling further prediction over an environment. However, 2D-based studies are both oriented towards short-term and long-term applications and therefore provide a background for decision making. Accordingly, thermal information can be used to monitor frost in a crop (Yuan and Choi, 2021), evaluate crop water stress (Qiu et al., 2021; Zhou et al., 2021), detect diseases on plants (Poblete et al., 2021, 2020a; Zarco-Tejada et al., 2018), such as the well-known Xylella Fastidiosa, as well as for plant phenotyping (Xu et al., 2021).

Fig. 14 shows the number of publications concerning 2D and 3D applications of thermal, multispectral and hyperspectral data sources, where thermal publications are slightly under the curve of hyperspectral research. Beyond the applications in forestry and agriculture, thermographic and multispectral information allows us to strengthen our knowledge about other natural environments, including volcanoes, glaciers, coastal or geothermal areas, as highlighted by (Guilbert et al., 2020). Given the relevance of simulation and prediction on emerging technologies (Angın et al., 2020; Chaux et al., 2021), thermal information is expected to represent a frequent data source for the monitoring of urban and natural environments. However, it is more likely to be applied on multi-source approaches along with visible, multispectral and hyperspectral captures, as it is commonly regarded as a complementary data source rather than the main data source (Lorenzo Comba et al., 2019; Hosoi et al., 2019; López et al., 2021a; Neale et al., 2011a; Xu et al., 2021).

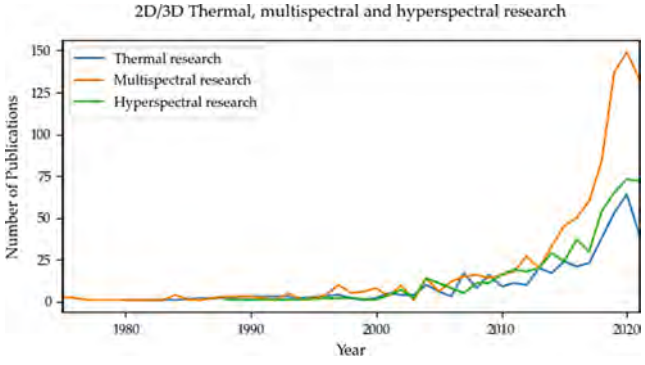

Fig. 14. Research concerning the three described data sources over a timeline from 1975 to 2021. The number of publications in recent years has experienced a significant increase with respect to previous periods.

Combining photogrammetric point clouds with hyperspectral data is a subject addressed in several studies. To map the damage of the European spruce bark beetle (*Ips typographus* L.) at the tree level, Näsi et al. (2015) developed an approach to analyzing spectral differences using UAV-based photogrammetry and HSI. The photogrammetric processing enabled to generate simultaneously dense point clouds using hyperspectral RGB-similar bands. For the remaining bands, a matching procedure is applied. Individual tree identification from the dense point cloud showed an accuracy of approximately 75%. As for classification, 76% and 90% as overall accuracies were obtained, respectively, when considering three classes (healthy, infested, dead) and two classes (healthy and dead). Demonstrating the potential of extracting forest health indicators in a bark beetle outbreak scenario. Following an identical data integration methodology, Nevalainen et al. (2017) addressed the use of UAV-based photogrammetric dense point clouds from RGB imagery along with HSI for individual tree detection and species classification in a boreal forest. Hyperspectral data were used alongside photogrammetric point clouds generated from RGB imagery. Both spectral and 3D point cloud features were used in the classification procedure where multiple classifiers were tested. The accuracy of the individual tree identification from point cloud data ranged from 40% to 95%, depending on the analyzed area. As for the species classification 95% overall accuracy was obtained in the random forest multilayer perceptron classifiers. The authors state that UAV-based hyperspectral 3D remote sensing was successful even in challenging conditions and the methods can serve as a tool for automatic remote sensing in environmental monitoring tasks. Saarinen et al. (2018) implemented the individual tree crown approaches to estimate plot-level biodiversity indicators in the boreal forest, by merging structural metrics from

photogrammetric RGB dense point clouds along with spectral features and vegetation indices derived from HSI. It was possible to assess the structural diversity with the integration of three-dimensional and spectral information, which can be suitable for biodiversity monitoring. In Cao et al. (2018) wetland ecosystems were monitored for mapping mangrove species using UAV-based snapshot HSI and digital surface models. Likewise, in Sothe et al. (2019) tree species classification (12) was performed in a Brazilian subtropical forest including photogrammetric RGB data along with HSI Li et al. (2017) showed that by using digital surface models and improvement in the mapping of wetland species is verified instead of using hyperspectral push-broom data only, misclassifications were reduced when considering height information. Nezami et al. (2020) performed the classification of tree species (pine, spruce and birch) using 3D CNNs trained with HSI UAV-based data and RGB sensors. The different extracted features were evaluated when used together or separated (spectral bands; red green blue and CHM). The combination of hyperspectral and RGB bands showed the best performance, outperforming RGB-only datasets. In this case, the improvements of CHM inclusion did not provide an added value for the tree species classification.

UAV-based LiDAR and hyperspectral data fusion is addressed in some forestry studies. Sankey et al. (2017) explored UAV-based LiDAR and push-broom hyperspectral data fusion for forest monitoring. The available LiDAR data were used to estimate individual tree height and crown diameter as well as total tree canopy cover and tree density in 10 m cells. HSI enabled to obtaining of spectral signatures for the vegetation subjected to analysis, contributing to better vegetation discrimination. A similar approach was applied by Sankey et al. (2018) for semi-arid land vegetation monitoring, LiDAR and HSI fusion enabled to the characterization of vegetation canopy structure along with the spectral signatures of each species. In both studies, LiDAR and HSI fusion showed the best overall accuracy for the classification of vegetation species and cover types than HSI data alone. Lin et al. (2019b) used HSI from a push-broom sensor and LiDAR data for the detection of pine shoot beetle (*Tomicus* spp.) stress at individual tree-level using a random forest classifier. The data from each sensor was evaluated by performing the classification separately and combining data from both sensors. To estimate the shoot damage ratio, the LiDAR data had a better performance than HSI data, but the best results were obtained when combining data from both sensors.

Regarding studies in agricultural crops, HSI and 3D information is mainly employed for the estimation of biomass and yield. Aasen et al. (2015) proposed a method to generate digital surface models from UAV-based HSI acquired using snapshot sensors. The processing pipeline has three stages. The first relies on the pre-processing of each cube and performing the radiometric calibration. Then photogrammetric processing is carried out to generate georeferenced point clouds and to compute a DSM and DTM of the entire surveyed area and orthorectified images for each acquired cube. The final step relies on the mosaicking of the orthorectified imagery in a geographical information system. Then, a hyperspectral digital surface model is created, connecting hyperspectral information in the 3D space. The 3D hyperspectral information was evaluated in a barley field. Regarding plant height, $R2 = 0.70$ was obtained with the 3D model underestimating approximately 0.19 m. The authors state that their approach can be applied to other image-frame sensors on the condition that each individual band from the data cube is spatially co-registered with each other. By combining spectral signatures and point cloud data Honkavaara et al. (2012) showed the possibility to estimate biomass in wheat and barley by training a support vector regression classifier. Yue et al. (2018) used a UAV-based snapshot hyperspectral sensor to estimate different crop parameters (leaf area index and above-ground biomass) in winter wheat in different epochs. These crop parameters were estimated by combining the vegetation indices and crop height models (CSMs) via linear and exponential equations, random forest, and partial least squares regression. Näsi et al. (2018) used HSI and photogrammetric 3D data for estimating several crop-related parameters (fresh and dry biomass and nitrogen amount) of barley and grass silage site. The orientations of the HSI bands that were not included in the photogrammetric processing were obtained by using a 3D band registration method for frame format hyperspectral which can be performed in complex forestry environments (Honkavaara et al., 2017). The method showed a sub-pixel band registration error. A random forest was used for regression. The best results in biomass estimation were obtained when integrating hyperspectral and 3D features, while for nitrogen content estimation the use of hyperspectral features only showed the best results. Above-ground biomass was better estimated when combining crop height and vegetation indices. In Li et al. (2020a) the combination of UAV-based push-broom HSI and height models from an RGB sensor is explored to perform above-ground biomass estimation and yield prediction in potato crops. Vanegas et al. (2018) proposed a methodology relying on UAV-based RGB, multispectral and hyperspectral data for plant pest surveillance, as a case study, phylloxera (*Daktulosphaira vitifoliae* Fitch) detection in vineyards. In this case, the hyperspectral data were compared with plant-height vigor maps generated from the 3D information retrieved from the digital elevation maps computed from the photogrammetric processing of the RGB data, by analyzing only pixels belonging to grapevines to assess the correlation of different vegetation indices and spectral signatures with vigor levels.

Deng et al. (2018b) evaluated the radiometric and geometric performance of a UAV-based hyperspectral image system at different spatial resolutions by analyzing a set of targets in what respects to its reflectance and geometry changes from data acquired from 30 m to 120 m. Despite not addressing 3D environments, this study provides a set of methods and directions towards the selection of the appropriate spatial resolution for UAV-based HSI acquisition with snapshot sensors, increasing operational efficiency.

6. Conclusions

Nowadays, multispectral and LiDAR data fusion that provides a combination of spectral and 3D information is in serious demand in many fields. With the development of monitoring technology, how to effectively integrate multispectral, thermal and hyperspectral data with the 3D geometry of natural and urban scenarios has been one of the frontier problems. In this survey, the most relevant advances in multisensorial image fusion and 3D generation of multi-sensorial data are introduced.

Smaller sensors, better optics, cheaper cost, more efficient batteries, increased stabilization, intelligent image capturing, and the ability to include all these capabilities on fully autonomous UAVs is the future challenge in remote sensing. The research community is taking the opportunity and is testing and proposing new ways of producing usable datasets and associated processing and algorithms, improving actual and offering new applications in the fields of agriculture and forestry, but not only. These facts combined with constant advances in small UAV design and availability, and other sensors that go beyond RGB and broadband (e.g., hyperspectral), make-believe that both the quality and quantity of data to produce a usable 3D multiple-sources dataset of specific areas of interest will drastically increase in the near future. In this paper, we have presented different approaches allowing the exploitation of the capabilities brought by the combination of multiple data sources and 3D information in a data fusion context. 3D scene reconstruction capability from images and fusion of material surface spectra (RGB, thermal, multispectral and hyperspectral) have proven to be of great interest and are a hot spot in current research. Multiple existing methods for the 3D reconstruction were presented, depending on the type of data used and, mainly, on their resolution. The manipulation of multispectral and hyperspectral data is well established and essentially results from the translation of the methods used in RGB images. Still, it is quite different, in terms of processing the use of snapshot or pushbroom hyperspectral data (Jurado et al., 2021). The use of thermal data turns out to be a

completely different world. The reconstruction of 3D thermographic models was described as a process composed of several stages to extract reliable temperature information. To overcome the challenges posed by thermal imagery, a significant number of methodologies were previously proposed. Each category was individually presented, and the topmost relevant studies were highlighted. However, the use of thermal data is yet to spread to agriculture and forestry-related applications.

Finally, considering the huge amount of data needed to be processed, it is recommended to improve the computation capabilities using GPU-based systems. These would provide results in real-time taking advantage of efficient data transfer methods and 5G technology. Moreover, rapid advances in artificial intelligence techniques will enable new approaches to data fusion, improving computational results and performance.

Declaration of Competing Interest

The authors declare that they have no known competing financial interests or personal relationships that could have appeared to influence the work reported in this paper.

Acknowledgements

This work has been partially funded through the research project 1381202-GEU, PYC20-RE-005-UJA, IEG-2021, which are co-financed with the Junta de Andalucía, Instituto de Estudios Gienneses and the European Union FEDER funds, as well as by the Spanish Ministry of Science, Innovation and Universities via the doctoral grant for the second author (FPU19/00100). Moreover, this research activity was supported by –"DATI - Digital Agriculture Technologies for Irrigation efficiency" project. PRIMA – Partnership for Research and Innovation in the Mediterranean Area, (Research and Innovation activities), financed by the states participating in the PRIMA partnership and by the European Union, through Horizon 2020 and by FCT – Portuguese Foundation for Science and Technology, under the project UIDB/04033/2020.

References

Aasen, H., Burkart, A., Bolten, A., Bareth, G., 2015. Generating 3D hyperspectral information with lightweight UAV snapshot cameras for vegetation monitoring: from camera calibration to quality assurance. ISPRS J. Photogramm. Remote Sens. 108, 245–259. https://doi.org/10.1016/j.isprsjprs.2015.08.002.

Abady, L., Barni, M., Garzelli, A., Tondi, B., 2020. GAN generation of synthetic multispectral satellite images, in: Image and Signal Processing for Remote Sensing XXVI. In: Presented at the Image and Signal Processing for Remote Sensing XXVI, pp. 122–133. https://doi.org/10.1117/12.2575765.

Adán, A., Prado, T., Prieto, S.A., Quintana, B., 2017. Fusion of thermal imagery and LiDAR data for generating TBIM models. In: in: 2017 IEEE SENSORS. Presented at the 2017 IEEE SENSORS, pp. 1–3. https://doi.org/10.1109/ICSENS.2017.8234261.

Adán, A., Quintana, B., Aguilar, J.G., Pérez, V., Castilla, F.J., 2020. Towards the use of 3D thermal models in constructions. Sustain. Switz. 12, 1–13. https://doi.org/10.3390/su12208521.

Adão, T., Hruška, J., Pádua, L., Bessa, J., Peres, E., Morais, R., Sousa, J.J., 2017. Hyperspectral imaging: a review on UAV-based sensors, data processing and applications for agriculture and forestry. Remote Sens. 9, 1110. https://doi.org/10.3390/rs9111110.

Ahmad, U., Alvino, A., Marino, S., 2021. A review of crop water stress assessment using remote sensing. Remote Sens. 13, 4155. https://doi.org/10.3390/rs13204155.

Alfredo Osornio-Rios, R., Antonino-Daviu, J.A., de Jesus Romero-Troncoso, R., 2019. Recent industrial applications of infrared thermography: a review. IEEE Trans. Ind. Inform. 15, 615–625. https://doi.org/10.1109/TII.2018.2884738.

de Almeida, D.R.A., Broadbent, E.N., Ferreira, M.P., Meli, P., Zambrano, A.M.A., Gorgens, E.B., Resende, A.F., de Almeida, C.T., do Amaral, C.H., Corte, A.P.D., Silva, C.A., Romanelli, J.P., Prata, G.A., de Almeida Papa, D., Stark, S.C., Valbuena, R., Nelson, B.W., Guillemot, J., Féret, J.-B., Chazdon, R., Brancalion, P.H. S., 2021. Monitoring restored tropical forest diversity and structure through UAV-borne hyperspectral and lidar fusion. Remote Sens. Environ. 264 https://doi.org/10.1016/j.rse.2021.112582.

Angel, Y., Turner, D., Parkes, S., Malbeteau, Y., Lucieer, A., McCabe, M.F., 2020. Automated Georectification and Mosaicking of UAV-Based Hyperspectral Imagery from Push-Broom Sensors. Remote Sens. 12, 34. https://doi.org/10.3390/rs12010034.

Angın, P., Anisi, M.H., Goksel, F., Gursoy, C., Buyukgulcu, A., 2020. AgriLoRa: A Digital Twin Framework for Smart Agriculture.

Antón, D., Amaro-Mellado, J.-L., 2021. Engineering graphics for thermal assessment: 3D thermal data visualisation based on infrared thermography, GIS and 3D point cloud processing software. Symmetry 13, 1–20. https://doi.org/10.3390/sym13020335.

Astor, T., Dayananda, S., Nautiyal, S., Wachendorf, M., 2020. Vegetable crop biomass estimation using hyperspectral and RGB 3D UAV data. Agronomy 10, 1600. https://doi.org/10.3390/agronomy10101600.

Ballouch, Z., Hajji, R., Ettarid, M., 2022. Toward a Deep Learning Approach for Automatic Semantic Segmentation of 3D Lidar Point Clouds in Urban Areas. In: Barramou, F., El Brirchi, E.H., Mansouri, K., Dehbi, Y. (Eds.), Geospatial Intelligence: Applications and Future Trends, Advances in Science, Technology & Innovation. Springer International Publishing, Cham, pp. 67–77. https://doi.org/10.1007/978-3-030-80458-9_6.

Behmann, J., Mahlein, A.-K., Paulus, S., Dupuis, J., Kuhlmann, H., Oerke, E.-C., Plümer, L., 2016. Generation and application of hyperspectral 3D plant models: methods and challenges. Mach. Vis. Appl. 27, 611–624. https://doi.org/10.1007/s00138-015-0716-8.

Behmann, J., Mahlein, A.-K., Paulus, S., Kuhlmann, H., Oerke, E.-C., Plümer, L., 2015. Calibration of hyperspectral close-range pushbroom cameras for plant phenotyping. ISPRS J. Photogramm. Remote Sens. 106, 172–182. https://doi.org/10.1016/j.isprsjprs.2015.05.010.

Bennis, A., Bombardier, V., Thiriet, P., Brie, D., 2013. Contours based approach for thermal image and terrestrial point cloud registration. In: The International Archives of the Photogrammetry, Remote Sensing and Spatial Information Sciences. Presented at the XXIV International CIPA Symposium (Volume XL-5/W2) - 6 September 2013, Strasbourg, France, Copernicus GmbH, pp. 97–101. https://doi.org/10.5194/isprsarchives-XL-5-W2-97-2013.

Benson, M.L., Pierce, L., Bergen, K., Sarabandi, K., 2021. Model-based estimation of forest canopy height and biomass in the Canadian boreal forest using radar, LiDAR, and optical remote sensing. IEEE Trans. Geosci. Remote Sens. 59, 4635–4653. https://doi.org/10.1109/TGRS.2020.3018638.

Boesch, R., 2017. Thermal remote sensing with UAV-based workflows. In: The International Archives of the Photogrammetry, Remote Sensing and Spatial Information Sciences. Presented at the International Conference on Unmanned Aerial Vehicles in Geomatics (Volume XLII-2/W6) - 4–7 September 2017, Bonn, Germany, Copernicus GmbH, pp. 41–46. https://doi.org/10.5194/isprs-archives-XLII-2-W6-41-2017.

Bolton, D.K., Tompalski, P., Coops, N.C., White, J.C., Wulder, M.A., Hermosilla, T., Queinnec, M., Luther, J.E., van Lier, O.R., Fournier, R.A., Woods, M., Treitz, P.M., van Ewijk, K.Y., Graham, G., Quist, L., 2020. Optimizing Landsat time series length for regional mapping of lidar-derived forest structure. Remote Sens. Environ. 239 https://doi.org/10.1016/j.rse.2020.111645.

Briechle, S., Krzystek, P., Vosselman, G., 2020. Classification of tree species and standing dead trees by fusing UAV-based lidar data and multispectral imagery in the 3D deep neural network PointNet++. ISPRS Ann. Photogramm. Remote Sens. Spat. Inf. Sci. 2, 203–210.

Bruning, B., Berger, B., Lewis, M., Liu, H., Garnett, T., 2020. Approaches, applications, and future directions for hyperspectral vegetation studies: An emphasis on yield-limiting factors in wheat. Plant Phenome J. 3, e20007 https://doi.org/10.1002/ppj2.20007.

Cao, C., Preda, M., Zaharia, T., 2019. 3D Point Cloud Compression: A Survey. In: The 24th International Conference on 3D Web Technology, Web3D '19. Association for Computing Machinery, New York, NY, USA, pp. 1–9. https://doi.org/10.1145/3329714.3338130.

Cao, J., Leng, W., Liu, K., Liu, L., He, Z., Zhu, Y., 2018. Object-based mangrove species classification using unmanned aerial vehicle hyperspectral images and digital surface models. Remote Sens. 10, 89. https://doi.org/10.3390/rs10010089.

Chakhvashvili, E., Siegmann, B., Bendig, J., Rascher, U., 2021. Comparison of reflectance calibration workflows for a UAV-mounted multi-camera array system. In: 2021 IEEE International Geoscience and Remote Sensing Symposium IGARSS. Presented at the 2021 IEEE International Geoscience and Remote Sensing Symposium IGARSS, pp. 8225–8228. https://doi.org/10.1109/IGARSS47720.2021.9555143.

Chan, Y.K., Koo, V.C., Choong, E.H.K., Lim, C.S., 2021. The Drone Based Hyperspectral Imaging System for Precision Agriculture. NVEO - Nat. VOLATILES Essent. OILS J. NVEO 5561–5573.

Chauhan, S., Darvishzadeh, R., Boschetti, M., Pepe, M., Nelson, A., 2019. Remote sensing-based crop lodging assessment: Current status and perspectives. ISPRS J. Photogramm. Remote Sens. 151, 124–140. https://doi.org/10.1016/j.isprsjprs.2019.03.005.

Chaux, J.D., Sanchez-Londono, D., Barbieri, G., 2021. A Digital Twin Architecture to Optimize Productivity within Controlled Environment Agriculture. Appl. Sci. 11, 8875. https://doi.org/10.3390/app11198875.

Clamens, T., Alexakis, G., Duverne, R., Seulin, R., Fauvet, E., Fofi, D., 2021. Real-time multispectral image processing and registration on 3D point cloud for vineyard analysis. In: 16th International Conference on Computer Vision Theory and Applications. Vienna, Austria. https://doi.org/10.5220/0010266203880398.

Clarkson, G., Luo, S., Fuentes, R., 2017. Thermal 3D modelling. ISARC Proc. 493–499.

Cohen-Steiner, D., Da, F., 2004. A greedy delaunay based surface reconstruction algorithm. Vis. Comput. 20, 4–16. https://doi.org/10.1007/s00371-003-0217-z.

Comba, L., Biglia, A., Aimonino, D.R., Barge, P., Tortia, C., Gay, P., 2019. 2D and 3D data fusion for crop monitoring in precision agriculture. In: 2019 IEEE International Workshop on Metrology for Agriculture and Forestry (MetroAgriFor). Presented at the 2019 IEEE International Workshop on Metrology for Agriculture and Forestry (MetroAgriFor), pp. 62–67. https://doi.org/10.1109/MetroAgriFor.2019.8909219.

Comba, L., Biglia, A., Ricauda Aimonino, D., Gay, P., 2018. Unsupervised detection of vineyards by 3D point-cloud UAV photogrammetry for precision agriculture.

Comput. Electron. Agric. 155, 84–95. https://doi.org/10.1016/j.compag.2018.10.005.
Correa, E.S., Calderon, F., Colorado, J.D., 2020. GFkuts: A novel multispectral image segmentation method applied to precision agriculture, In: 2020 Virtual Symposium in Plant Omics Sciences (OMICAS). IEEE, pp. 1–6.
Cunha, J., Gaspar, P.D., Assunção, E., Mesquita, R., 2021. Prediction of the Vigor and Health of Peach Tree Orchard. In: in: International Conference on Computational Science and Its Applications. Springer, pp. 541–551.
Dachsbacher, C., Stamminger, M., 2003. Translucent shadow maps. Render. Tech. 2003, 197–201.
Dahaghin, M., Samadzadegan, F., Dadras Javan, F., 2019. 3D thermal mapping of building roofs based on fusion of thermal and visible point clouds in uav imagery. In: Presented at the International Archives of the Photogrammetry, Remote Sensing and Spatial Information Sciences - ISPRS Archives, pp. 271–277. https://doi.org/10.5194/isprs-archives-XLII-4-W18-271-2019.
Dahaghin, M., Samadzadegan, F., Dadrass Javan, F., 2021. Precise 3D extraction of building roofs by fusion of UAV-based thermal and visible images. Int. J. Remote Sens. 42, 7002–7030. https://doi.org/10.1080/01431161.2021.1951875.
Dai, W., Yang, B., Dong, Z., Shaker, A., 2018. A new method for 3D individual tree extraction using multispectral airborne LiDAR point clouds. ISPRS J. Photogramm. Remote Sens. 144, 400–411. https://doi.org/10.1016/j.isprsjprs.2018.08.010.
Dalponte, M., Marzini, S., Solano-Correa, Y.T., Tonon, G., Vescovo, L., Gianelle, D., 2020. Mapping forest windthrows using high spatial resolution multispectral satellite images. Int. J. Appl. Earth Obs. Geoinformation 93, 102206. https://doi.org/10.1016/j.jag.2020.102206.
Dash, J.P., Watt, M.S., Paul, T.S., Morgenroth, J., Pearse, G.D., 2019. Early detection of invasive exotic trees using UAV and manned aircraft multispectral and LiDAR Data. Remote Sens. 11, 1812.
de Oca, A.M., Flores, G., 2021. A UAS equipped with a thermal imaging system with temperature calibration for Crop Water Stress Index computation. In: in: 2021 International Conference on Unmanned Aircraft Systems (ICUAS). Presented at the 2021 International Conference on Unmanned Aircraft Systems (ICUAS), pp. 714–720. https://doi.org/10.1109/ICUAS51884.2021.9476863.
Debevec, P., Yu, Y., Borshukov, G., 1998. Efficient view-dependent image-based rendering with projective texture-mapping. Eurographics Workshop on Rendering Techniques. Springer 105–116.
Deng, L., Mao, Z., Li, X., Hu, Z., Duan, F., Yan, Y., 2018a. UAV-based multispectral remote sensing for precision agriculture: A comparison between different cameras. ISPRS J. Photogramm. Remote Sens. 146, 124–136.
Deng, L., Yan, Y., Gong, H., Duan, F., Zhong, R., 2018b. The effect of spatial resolution on radiometric and geometric performances of a UAV-mounted hyperspectral 2D imager. ISPRS J. Photogramm. Remote Sens. 144, 298–314. https://doi.org/10.1016/j.isprsjprs.2018.08.002.
Dino, I.G., Sari, A.E., Iseri, O.K., Akin, S., Kalfaoglu, E., Erdogan, B., Kalkan, S., Alatan, A. A., 2020. Image-based construction of building energy models using computer vision. Autom. Constr. 116, 103231.
Du, X., Wan, L., Cen, H., Chen, S., Zhu, J., Wang, H., He, Y., 2020. Multi-temporal monitoring of leaf area index of rice under different nitrogen treatments using UAV images. Int. J. Precis. Agric Aviat. 3.
Dua, Y., Kumar, V., Singh, R.S., 2020. Comprehensive review of hyperspectral image compression algorithms. Opt. Eng. 59, 090902 https://doi.org/10.1117/1.OE.59.9.090902.
Effiom, A.E., van Leeuwen, L.M., Nyktas, P., Okojie, J.A., Erdbrügger, J., 2019. Combining unmanned aerial vehicle and multispectral Pleiades data for tree species identification, a prerequisite for accurate carbon estimation. J. Appl. Remote Sens. 13.
Everitt, C., 2001. Interactive order-independent transparency. White Pap. NVIDIA 2, 7.
Fang, J., Wang, X., Zhu, T., Liu, X., Zhang, X., Zhao, D., 2019. A Novel Mosaic Method for UAV-Based Hyperspectral Images. In: IGARSS 2019–2019 IEEE International Geoscience and Remote Sensing Symposium. Presented at the IGARSS 2019–2019 IEEE International Geoscience and Remote Sensing Symposium, pp. 9220–9223. https://doi.org/10.1109/IGARSS.2019.8900057.
Feng, Z., Chen, Y., Hakala, T., Hyyppä, J., 2016. Range calibration of airborne profiling radar used in forest inventory. In: 2016 IEEE International Geoscience and Remote Sensing Symposium, IGARSS 2016 - Proceedings, IEEE International Geoscience and Remote Sensing Symposium Proceedings. IEEE, United States, pp. 6672–6675. https://doi.org/10.1109/IGARSS.2016.7730742.
Ferrera, M., Arnaubec, A., Istenič, K., Gracias, N., Bajjouk, T., 2021. Hyperspectral 3D Mapping of Underwater Environments. In: Presented at the Proceedings of the IEEE/CVF International Conference on Computer Vision, pp. 3703–3712.
Franzini, M., Ronchetti, G., Sona, G., Casella, V., 2019. Geometric and radiometric consistency of parrot sequoia multispectral imagery for precision agriculture applications. Appl. Sci. 9, 5314.
Gade, R., Moeslund, T.B., 2014. Thermal cameras and applications: a survey. Mach. Vis. Appl. 25, 245–262. https://doi.org/10.1007/s00138-013-0570-5.
Gadiraju, K.K., Ramachandra, B., Chen, Z., Vatsavai, R.R., 2020. In: Multimodal Deep Learning Based Crop Classification Using Multispectral and Multitemporal Satellite Imagery, in. Association for Computing Machinery, New York, NY, USA, pp. 3234–3242. https://doi.org/10.1145/3394486.3403375.
Gani, M.O., Kuiry, S., Das, A., Nasipuri, M., Das, N., 2021. Multispectral Object Detection with Deep Learning, in. In: International Conference on Computational Intelligence in Communications and Business Analytics. Springer, pp. 105–117.
Garzonio, R., Di Mauro, B., Colombo, R., Cogliati, S., 2017. Surface Reflectance and Sun-Induced Fluorescence Spectroscopy Measurements Using a Small Hyperspectral UAS. Remote Sens. 9, 472. https://doi.org/10.3390/rs9050472.
Ghamisi, P., Rasti, B., Yokoya, N., Wang, Q., Hofle, B., Bruzzone, L., Bovolo, F., Chi, M., Anders, K., Gloaguen, R., Atkinson, P.M., Benediktsson, J.A., 2019. Multisource and Multitemporal Data Fusion in Remote Sensing: A Comprehensive Review of the State of the Art. IEEE Geosci. Remote Sens. Mag. 7, 6–39. https://doi.org/10.1109/MGRS.2018.2890023.
Gómez, A., Randall, G., Facciolo, G., von Gioi, R.G., 2022. An experimental comparison of multi-view stereo approaches on satellite images. In: Presented at the Proceedings of the IEEE/CVF Winter Conference on Applications of Computer Vision, pp. 844–853.
González, O., Lizarraga, M.I., Karaman, S., Salas, J., 2019. Thermal Radiation Dynamics of Soil Surfaces with Unmanned Aerial Systems. In: Carrasco-Ochoa, J.A., Martínez-Trinidad, J.F., Olvera-López, J.A., Salas, J. (Eds.), Pattern Recognition, Lecture Notes in Computer Science. Springer International Publishing, Cham, pp. 183–192. https://doi.org/10.1007/978-3-030-21077-9_17.
Grechi, G., Fiorucci, M., Marmoni, G.M., Martino, S., 2021. 3D thermal monitoring of jointed rock masses through infrared thermography and photogrammetry. Remote Sens. 13, 957. https://doi.org/10.3390/rs13050957.
Griffiths, D., Boehm, J., 2019. Improving public data for building segmentation from Convolutional Neural Networks (CNNs) for fused airborne lidar and image data using active contours. ISPRS J. Photogramm. Remote Sens. 154, 70–83. https://doi.org/10.1016/j.isprsjprs.2019.05.013.
Gu, Y., Jin, X., Xiang, R., Wang, Q., Wang, C., Yang, S., 2020. UAV-based integrated multispectral-LiDAR imaging system and data processing. Sci. China Technol. Sci. 63, 1293–1301. https://doi.org/10.1007/s11431-019-1571-0.
Gui, S., Qin, R., 2021. Automated LoD-2 model reconstruction from very-high-resolution satellite-derived digital surface model and orthophoto. ISPRS J. Photogramm. Remote Sens. 181, 1–19. https://doi.org/10.1016/j.isprsjprs.2021.08.025.
Guilbert, V., Antoine, R., Heinkelé, C., Maquaire, O., Costa, S., Gout, C., Davidson, R., Sorin, J.-L., Beaucamp, B., Fauchard, C., 2020. Fusion of thermal and visible point clouds: application to the vaches noires landslide, Normandy, France. In: Presented at the International Archives of the Photogrammetry, Remote Sensing and Spatial Information Sciences - ISPRS Archives, pp. 227–232. https://doi.org/10.5194/isprs-archives-XLIII-B2-2020-227-2020.
Guimarães, N., Pádua, L., Marques, P., Silva, N., Peres, E., Sousa, J.J., 2020. Forestry remote sensing from unmanned aerial vehicles: a review focusing on the data processing and potentialities. Remote Sens. 12, 1046. https://doi.org/10.3390/rs12061046.
Guo, L., Chehata, N., Mallet, C., Boukir, S., 2011. Relevance of airborne lidar and multispectral image data for urban scene classification using Random Forests. ISPRS J. Photogramm. Remote Sens. 66, 56–66. https://doi.org/10.1016/j.isprsjprs.2010.08.007.
Ham, Y., Golparvar-Fard, M., 2013. An automated vision-based method for rapid 3D energy performance modeling of existing buildings using thermal and digital imagery. Adv. Eng. Inform. 27, 395–409. https://doi.org/10.1016/j.aei.2013.03.005.
Han, Y., Wang, S., Gong, D., Wang, Y., Wang, Y., Ma, X., 2020. State of the art in digital surface modelling from multi-view high-resolution satellite images. In: ISPRS Annals of the Photogrammetry, Remote Sensing and Spatial Information Sciences. Presented at the XXIV ISPRS Congress, Commission II (Volume V-2-2020) - 2020 edition, Copernicus GmbH, pp. 351–356. https://doi.org/10.5194/isprs-annals-V-2-2020-351-2020.
Heckbert, P.S., 1986. Survey of Texture Mapping. IEEE Comput. Graph. Appl. 6, 56–67. https://doi.org/10.1109/MCG.1986.276672.
Heckel, K., Urban, M., Schratz, P., Mahecha, M.D., Schmullius, C., 2020. Predicting forest cover in distinct ecosystems: the potential of multi-source Sentinel-1 and -2 data fusion. Remote Sens. 12, 302. https://doi.org/10.3390/rs12020302.
Hoegner, L., Abmayr, T., Tosic, D., Turzer, S., Stilla, U., 2018. Fusion of 3D point clouds with tir images for indoor scene reconstruction. In: The International Archives of the Photogrammetry, Remote Sensing and Spatial Information Sciences. Presented at the ISPRS TC I Mid-term Symposium Innovative Sensing – From Sensors to Methods and Applications (Volume XLII-1) - 10-12 October 2018, Karlsruhe, Germany, Copernicus GmbH, pp. 189–194. https://doi.org/10.5194/isprs-archives-XLII-1-189-2018.
Hoegner, Ludwig, Abmayr, T., Tosic, D., Turzer, S., Stilla, U., 2018. Fusion of TLS and RGB point clouds with TIR images for indoor mobile mapping. In: Presented at the 2018 Quantitative InfraRed Thermography, Berlin. https://doi.org/10.21611/qirt.2018.019.
Hoegner, L., Stilla, U., 2018. Mobile thermal mapping for matching of infrared images with 3D building models and 3D point clouds. Quant. InfraRed Thermogr. J. 15, 252–270. https://doi.org/10.1080/17686733.2018.1455129.
Hoegner, L., Tuttas, S., Stilla, U., 2016a. 3D building reconstruction and construction site monitoring from RGB and TIR image sets. In: in: 2016 12th IEEE International Symposium on Electronics and Telecommunications (ISETC). Presented at the 2016 12th IEEE International Symposium on Electronics and Telecommunications (ISETC), pp. 305–308. https://doi.org/10.1109/ISETC.2016.7781118.
Hoegner, L., Tuttas, S., Xu, Y., Eder, K., Stilla, U., 2016b. Evaluation of Methods for Coregistration and Fusion of Rpas-Based 3d Point Clouds and Thermal Infrared Images. ISPRS - Int. Arch. Photogramm. Remote Sens. Spat. Inf. Sci. 49B3, 241–246. https://doi.org/10.5194/isprs-archives-XLI-B3-241-2016.
Honkavaara, E., Kaivosoja, J., Mäkynen, J., Pellikka, I., Pesonen, L., Saari, H., Salo, H., Hakala, T., Marklelin, L., Rosnell, T., 2012. HYPERSPECTRAL reflectance signatures and point clouds for precision agriculture by light weight UAV imaging system. In: ISPRS Annals of the Photogrammetry, Remote Sensing and Spatial Information Sciences. Presented at the XXII ISPRS Congress, Technical Commission VII (Volume I-7) - 25 August – 01 September 2012, Melbourne, Australia, Copernicus GmbH, pp. 353–358. https://doi.org/10.5194/isprsannals-I-7-353-2012.

Honkavaara, E., Rosnell, T., Oliveira, R., Tommaselli, A., 2017. Band registration of tuneable frame format hyperspectral UAV imagers in complex scenes. ISPRS J. Photogramm. Remote Sens. 134, 96–109. https://doi.org/10.1016/j.isprsjprs.2017.10.014.

Horstrand, P., Guerra, R., Rodríguez, A., Díaz, M., López, S., López, J Fco, 2019. A UAV platform based on a hyperspectral sensor for image capturing and on-board processing. IEEE Access 7, 66919–66938. https://doi.org/10.1109/ACCESS.2019.2913957.

Hosoi, F., Umeyama, S., Kuo, K., 2019. Estimating 3D chlorophyll content distribution of trees using an image fusion method between 2D camera and 3D portable scanning lidar. Remote Sens. 11 https://doi.org/10.3390/rs11182134.

Hou, Y., Volk, R., Chen, M., Soibelman, L., 2021. Fusing tie points' RGB and thermal information for mapping large areas based on aerial images: A study of fusion performance under different flight configurations and experimental conditions. Autom. Constr. 124, 103554 https://doi.org/10.1016/j.autcon.2021.103554.

Huang, Y., Chiang, C.-H., Hsu, K.-T., 2018. Combining the 3D model generated from point clouds and thermography to identify the defects presented on the facades of a building. In: Nondestructive Characterization and Monitoring of Advanced Materials, Aerospace, Civil Infrastructure, and Transportation XII. Presented at the Nondestructive Characterization and Monitoring of Advanced Materials, Aerospace, Civil Infrastructure, and Transportation XII, International Society for Optics and Photonics, p. 105990G. https://doi.org/10.1117/12.2297656.

Hutton, J.J., Lipa, G., Baustian, D., Sulik, J., Bruce, R.W., 2020. High accuracy direct georeferencing of the altum multi-spectral uav camera and its application to high throughput plant phenotyping. Int. Arch. Photogramm. Remote Sens. Spat. Inf. Sci. 43, 451–456.

Iglhaut, J., Cabo, C., Puliti, S., Piermattei, L., O'Connor, J., Rosette, J., 2019. Structure from motion photogrammetry in forestry: a review. Curr. For. Rep. 5, 155–168. https://doi.org/10.1007/s40725-019-00094-3.

INPE/CBERS [WWW Document], 2021. URL http://www.cbers.inpe.br/ (accessed 9.13.21).

Isgró, M.A., Basallote, M.D., Barbero, L., 2021. Unmanned aerial system-based multispectral water quality monitoring in the iberian pyrite belt (SW Spain). Mine Water Environ. 1–12.

Iwaszczuk, D., Stilla, U., 2017. Camera pose refinement by matching uncertain 3D building models with thermal infrared image sequences for high quality texture extraction. ISPRS J. Photogramm. Remote Sens. 132, 33–47. https://doi.org/10.1016/j.isprsjprs.2017.08.006.

James, D., Collin, A., Mury, A., Letard, M., Guillot, B., 2021. UAV Multispectral Optical Contribution to Coastal 3D Modelling. In: in: 2021 IEEE International Geoscience and Remote Sensing Symposium IGARSS. Presented at the 2021 IEEE International Geoscience and Remote Sensing Symposium IGARSS, pp. 7951–7954. https://doi.org/10.1109/IGARSS47720.2021.9553865.

Jarząbek-Rychard, M., Lin, D., Maas, H.-G., 2020. Supervised Detection of Façade Openings in 3D Point Clouds with Thermal Attributes. Remote Sens. 12, 543. https://doi.org/10.3390/rs12030543.

Javadnejad, F., Gillins, D.T., Parrish, C.E., Slocum, R.K., 2020. A photogrammetric approach to fusing natural colour and thermal infrared UAS imagery in 3D point cloud generation. Int. J. Remote Sens. 41, 211–237. https://doi.org/10.1080/01431161.2019.1641241.

Jayakumari, R., Nidamanuri, R.R., Ramiya, A.M., 2021. Object-level classification of vegetable crops in 3D LiDAR point cloud using deep learning convolutional neural networks. Precis. Agric. 22, 1617–1633. https://doi.org/10.1007/s11119-021-09803-0.

Jeong, J.H., Jae, J.Y., Wang, L.J., Hong, O.J., 2021. Dense thermal 3d point cloud generation of building envelope by drone-based photogrammetry. J. Korean Soc. Surv. Geod. Photogramm. Cartogr. 39, 73–79. https://doi.org/10.7848/ksgpc.2021.39.2.73.

Jiang, S., Jiang, C., Jiang, W., 2020. Efficient structure from motion for large-scale UAV images: a review and a comparison of SfM tools. ISPRS J. Photogramm. Remote Sens. 167, 230–251. https://doi.org/10.1016/j.isprsjprs.2020.04.016.

Jing, Z., Guan, H., Zhao, P., Li, D., Yu, Y., Zang, Y., Wang, H., Li, J., 2021. Multispectral LiDAR point cloud classification using SE-PointNet++. Remote Sens. 13, 2516. https://doi.org/10.3390/rs13132516.

Jurado, J.M., 2020. Spectral Characterization and Semantic Segmentation of Complex 3D models in Natural Environments.

Jurado, J.M., Cárdenas, J.L., Ogayar, C.J., Ortega, L., Feito, F.R., 2020a. Semantic segmentation of natural materials on a point cloud using spatial and multispectral features. Sensors 20, 2244. https://doi.org/10.3390/s20082244.

Jurado, J.M., Ortega, L., Cubillas, J.J., Feito, F.R., 2020b. Multispectral mapping on 3D models and multi-temporal monitoring for individual characterization of olive trees. Remote Sens. 12, 1106. https://doi.org/10.3390/rs12071106.

Jurado, J.M., Pádua, L., Hruška, J., Feito, F.R., Sousa, J.J., 2021. An Efficient method for generating UAV-based hyperspectral mosaics using push-broom sensors. IEEE J. Sel. Top. Appl. Earth Obs. Remote Sens. 14, 6515–6531. https://doi.org/10.1109/JSTARS.2021.3088945.

Jurado, J.M., Ramos, M.I., Enríquez, C., Feito, F.R., 2020c. The Impact of canopy reflectance on the 3D structure of individual trees in a Mediterranean forest. Remote Sens. 12 https://doi.org/10.3390/rs12091430.

Juszczyk, J.M., Wijata, A., Czajkowska, J., Krecichwost, M., Rudzki, M., Biesok, M., Pyciński, B., Majewski, J., Kostecki, J., Pietka, E., 2021. Wound 3D geometrical feature estimation using poisson reconstruction. IEEE Access 9, 7894–7907. https://doi.org/10.1109/ACCESS.2020.3035125.

Kalisperakis, I., Stentoumis, C., Grammatikopoulos, L., Karantzalos, K., 2015. Leaf area index estimation in vineyards from UAV hyperspectral data, 2D image mosaics and 3D canopy surface models. Int. Arch. Photogramm. Remote Sens. Spat. Inf. Sci. 40, 299.

Keshk, H.M., Yin, X.-C., 2017. Satellite super-resolution images depending on deep learning methods: a comparative study. In: 2017 IEEE International Conference on Signal Processing, Communications and Computing (ICSPCC). Presented at the 2017 IEEE International Conference on Signal Processing, Communications and Computing (ICSPCC), pp. 1–7. https://doi.org/10.1109/ICSPCC.2017.8242625.

Kniaz, V.V., Mizginov, V.A., 2018. Thermal Texture Generation and 3d Model Reconstruction Using SFM and Gan. ISPRS - Int. Arch. Photogramm. Remote Sens. Spat. Inf. Sci. 422, 519–524. https://doi.org/10.5194/isprs-archives-XLII-2-519-2018.

Kong, Y., Leung, H., Zhang, B., Xing, S., Chen, Y., 2018. 3-D point cloud reconstruction of infrared images based on improved structure from motion. In: Presented at the Proceedings - 2018 2nd European Conference on Electrical Engineering and Computer Science, EECS 2018, pp. 307–310. https://doi.org/10.1109/EECS.2018.00063.

Kotaridis, I., Lazaridou, M., 2021. Remote sensing image segmentation advances: a meta-analysis. ISPRS J. Photogramm. Remote Sens. 173, 309–322. https://doi.org/10.1016/j.isprsjprs.2021.01.020.

Lafi, G.A., Zhu, Z., Dawood, T., Zayed, T., 2017. 3D Thermal and spatial modeling of a subway tunnel: a case study 386–394. https://doi.org/10.1061/9780784480823.046.

Landmann, M., Heist, S., Dietrich, P., Lutzke, P., Gebhart, I., Kühmstedt, P., Notni, G., 2019. Multimodal sensor: high-speed 3D and thermal measurement. Presented at the Proceedings of SPIE - The International Society for Optical Engineering. https://doi.org/10.1117/12.2531950.

Landsat 9, n.d.

Lechner, A.M., Foody, G.M., Boyd, D.S., 2020. Applications in remote sensing to forest ecology and management. One Earth 2, 405–412. https://doi.org/10.1016/j.oneear.2020.05.001.

Lee, K., Kim, K., Lee, S.-G., Kim, Y., 2020. Determination of the Normalized Difference Vegetation Index (NDVI) with Top-of-Canopy (TOC) reflectance from a KOMPSAT-3A image using Orfeo ToolBox (OTB) extension. ISPRS Int. J. Geo-Inf. 9, 257.

Li, B., Xu, X., Zhang, L., Han, J., Bian, C., Li, G., Liu, J., Jin, L., 2020a. Above-ground biomass estimation and yield prediction in potato by using UAV-based RGB and hyperspectral imaging. ISPRS J. Photogramm. Remote Sens. 162, 161–172. https://doi.org/10.1016/j.isprsjprs.2020.02.013.

Li, D., Song, Z., Quan, C., Xu, X., Liu, C., 2021. Recent advances in image fusion technology in agriculture. Comput. Electron. Agric. 191, 106491 https://doi.org/10.1016/j.compag.2021.106491.

Li, Q.S., Wong, F.K.K., Fung, T., 2017. Assessing the Utility of Uav-Borne Hyperspectral Image and Photogrammetry Derived 3d Data for Wetland Species Distribution Quick Mapping. ISPRS - Int. Arch. Photogramm. Remote Sens. Spat. Inf. Sci. 42W6, 209–215. https://doi.org/10.5194/isprs-archives-XLII-2-W6-209-2017.

Li, Y., Li, M., Liu, Z., Li, C., 2020b. Combining kriging interpolation to improve the accuracy of forest aboveground biomass estimation using remote sensing data. IEEE Access 8, 128124–128139. https://doi.org/10.1109/ACCESS.2020.3008686.

Lin, D., Jarzabek-Rychard, M., Tong, X., Maas, H.-G., 2019a. Fusion of thermal imagery with point clouds for building façade thermal attribute mapping. ISPRS J. Photogramm. Remote Sens. 151, 162–175. https://doi.org/10.1016/j.isprsjprs.2019.03.010.

Lin, Q., Huang, H., Wang, J., Huang, K., Liu, Y., 2019b. Detection of Pine Shoot Beetle (PSB) stress on pine forests at individual tree level using UAV-based hyperspectral imagery and lidar. Remote Sens. 11, 2540. https://doi.org/10.3390/rs11212540.

Liu, H., Bruning, B., Garnett, T., Berger, B., 2020. Hyperspectral imaging and 3D technologies for plant phenotyping: from satellite to close-range sensing. Comput. Electron. Agric. 175, 105621 https://doi.org/10.1016/j.compag.2020.105621.

Liu, H., Lee, S.-H., Chahl, J.S., 2018. Registration of multispectral 3D points for plant inspection. Precis. Agric. 19, 513–536. https://doi.org/10.1007/s11119-017-9536-3.

Lombardo, V., Pick, L., Spinetti, C., Tadeucci, J., Zakšek, K., 2020. Temperature and emissivity separation 'Draping'algorithm applied to hyperspectral infrared data. Remote Sens. 12, 2046.

López, A., Jurado, J.M., Ogayar, C.J., Feito, F.R., 2021a. A framework for registering UAV-based imagery for crop-tracking in Precision Agriculture. Int. J. Appl. Earth Obs. Geoinformation 97, 102274. https://doi.org/10.1016/j.jag.2020.102274.

López, A., Jurado, J.M., Ogayar, C.J., Feito, F.R., 2021b. An optimized approach for generating dense thermal point clouds from UAV-imagery. ISPRS J. Photogramm. Remote Sens. 182, 78–95. https://doi.org/10.1016/j.isprsjprs.2021.09.022.

López, A., Jurado, J.M., Padrón, E.J., Ogayar, C.J., Feito, F.R., 2021c. Comparison of GPU-based methods for handling point cloud occlusion. The Eurographics Association. https://doi.org/10.2312/ceig.20211364.

Lu, H., Fan, T., Ghimire, P., Deng, L., 2020. Experimental evaluation and consistency comparison of UAV multispectral minisensors. Remote Sens. 12, 2542.

Macher, H., Boudhaim, M., Grussenmeyer, P., Siroux, M., Landes, T., 2019. Combination of thermal and geometric information for BIM enrichment. In: Presented at the International Archives of the Photogrammetry, Remote Sensing and Spatial Information Sciences - ISPRS Archives, pp. 719–725. https://doi.org/10.5194/isprs-archives-XLII-2-W15-719-2019.

Maes, W.H., Huete, A.R., Steppe, K., 2017. Optimizing the processing of UAV-based thermal imagery. Remote Sens. 9, 476. https://doi.org/10.3390/rs9050476.

Maimaitijiang, M., Sagan, V., Sidike, P., Daloye, A.M., Erkbol, H., Fritschi, F.B., 2020. Crop monitoring using satellite/UAV data fusion and machine learning. Remote Sens. 12, 1357. https://doi.org/10.3390/rs12091357.

Main-Knorn, M., Pflug, B., Louis, J., Debaecker, V., Müller-Wilm, U., Gascon, F., 2017. Sen2Cor for sentinel-2. In: Image and Signal Processing for Remote Sensing XXIII. International Society for Optics and Photonics, p. 1042704.

Manzanera, J.A., García-Abril, A., Pascual, C., Tejera, R., Martín-Fernández, S., Tokola, T., Valbuena, R., 2016. Fusion of airborne LiDAR and multispectral sensors reveals synergic capabilities in forest structure characterization. GIScience Remote Sens. 53, 723–738. https://doi.org/10.1080/15481603.2016.1231605.

Maset, E., Fusiello, A., Crosilla, F., Toldo, R., Zorzetto, D., 2017. Photogrammetric 3D building reconstruction from thermal images. In: ISPRS Annals of the Photogrammetry, Remote Sensing and Spatial Information Sciences. Copernicus GmbH, Bonn, Germany, pp. 25–32. https://doi.org/10.5194/isprs-annals-IV-2-W3-25-2017.

Matese, A., Di Gennaro, S.F., Berton, A., 2017. Assessment of a canopy height model (CHM) in a vineyard using UAV-based multispectral imaging. Int. J. Remote Sens. 38, 2150–2160. https://doi.org/10.1080/01431161.2016.1226002.

Mathews, A.J., Jensen, J.L.R., 2013. Visualizing and quantifying vineyard canopy LAI Using an Unmanned Aerial Vehicle (UAV) collected high density structure from motion point cloud. Remote Sens. 5, 2164–2183. https://doi.org/10.3390/rs5052164.

Mäyrä, J., Keski-Saari, S., Kivinen, S., Tanhuanpää, T., Hurskainen, P., Kullberg, P., Poikolainen, L., Viinikka, A., Tuominen, S., Kumpula, T., Vihervaara, P., 2021. Tree species classification from airborne hyperspectral and LiDAR data using 3D convolutional neural networks. Remote Sens. Environ. 256, 112322 https://doi.org/10.1016/j.rse.2021.112322.

McManus, C., Tanure, C.B., Peripolli, V., Seixas, L., Fischer, V., Gabbi, A.M., Menegassi, S.R.O., Stumpf, M.T., Kolling, G.J., Dias, E., Costa, J.B.G., 2016. Infrared thermography in animal production: an overview. Comput. Electron. Agric. 123, 10–16. https://doi.org/10.1016/j.compag.2016.01.027.

Meister, D., Bittner, J., 2018. Parallel locally-ordered clustering for bounding volume hierarchy construction. IEEE Trans. Vis. Comput. Graph. 24, 1345–1353. https://doi.org/10.1109/TVCG.2017.2669983.

Mesas-Carrascosa, F.-J., de Castro, A.I., Torres-Sánchez, J., Triviño-Tarradas, P., Jiménez-Brenes, F.M., García-Ferrer, A., López-Granados, F., 2020. Classification of 3D point clouds using color vegetation indices for precision viticulture and digitizing applications. Remote Sens. 12, 317.

Metcalf, J.P., Olsen, R.C., 2016. Evaluation of terrestrial photogrammetric point clouds derived from thermal imagery. In: Thermosense: Thermal Infrared Applications XXXVIII. Presented at the Thermosense: Thermal Infrared Applications XXXVIII, SPIE, pp. 323–329. https://doi.org/10.1117/12.2224406.

Mitchell, J.J., Shrestha, R., Spaete, L.P., Glenn, N.F., 2015. Combining airborne hyperspectral and LiDAR data across local sites for upscaling shrubland structural information: lessons for HyspIRI. Remote Sens. Environ Special Issue on the Hyperspectral Infrared Imager (HyspIRI) 167, 98–110. https://doi.org/10.1016/j.rse.2015.04.015.

Mohandoss, T., Kulkarni, A., Northrup, D., Mwebaze, E., Alemohammad, H., 2020. Generating Synthetic Multispectral Satellite Imagery from Sentinel-2. ArXiv201203108 Cs Eess.

Müller, M.U., Ekhtiari, N., Almeida, R.M., Rieke, C., 2020. Super-resolution of multispectral satellite images using convolutional neural networks. ArXiv Prepr. ArXiv200200580.

Näsi, R., Honkavaara, E., Lyytikäinen-Saarenmaa, P., Blomqvist, M., Litkey, P., Hakala, T., Viljanen, N., Kantola, T., Tanhuanpää, T., Holopainen, M., 2015. Using UAV-based photogrammetry and hyperspectral imaging for mapping bark beetle damage at tree-level. Remote Sens. 7, 15467–15493. https://doi.org/10.3390/rs71115467.

Näsi, R., Viljanen, N., Kaivosoja, J., Alhonoja, K., Hakala, T., Markelin, L., Honkavaara, E., 2018. Estimating biomass and nitrogen amount of barley and grass using UAV and aircraft based spectral and photogrammetric 3D features. Remote Sens. 10, 1082. https://doi.org/10.3390/rs10071082.

Neale, C.M.U., Geli, H., Taghvaeian, S., Masih, A., Pack, R.T., Simms, R.D., Baker, M., Milliken, J.A., O'Meara, S., Witherall, A.J., 2011a. Estimating evapotranspiration of riparian vegetation using high resolution multispectral, thermal infrared and lidar data. In: Remote Sensing for Agriculture, Ecosystems, and Hydrology XIII. Presented at the Remote Sensing for Agriculture, Ecosystems, and Hydrology XIII, SPIE, pp. 254–262. https://doi.org/10.1117/12.903246.

Neale, C.M.U., Geli, H., Taghvaeian, S., Masih, A., Pack, R.T., Simms, R.D., Baker, M., Milliken, J.A., O'Meara, S., Witherall, A.J., 2011b. Estimating evapotranspiration of riparian vegetation using high resolution multispectral, thermal infrared and lidar data. In: Remote Sensing for Agriculture, Ecosystems, and Hydrology XIII. Presented at the Remote Sensing for Agriculture, Ecosystems, and Hydrology XIII, SPIE, pp. 254–262. https://doi.org/10.1117/12.903246.

Nevalainen, O., Honkavaara, E., Tuominen, S., Viljanen, N., Hakala, T., Yu, X., Hyyppä, J., Saari, H., Pölönen, I., Imai, N.N., Tommaselli, A.M.G., 2017. Individual tree detection and classification with UAV-based photogrammetric point clouds and hyperspectral imaging. Remote Sens. 9, 185. https://doi.org/10.3390/rs9030185.

Nezami, S., Khoramshahi, E., Nevalainen, O., Pölönen, I., Honkavaara, E., 2020. Tree species classification of drone hyperspectral and RGB imagery with deep learning convolutional neural networks. Remote Sens. 12, 1070. https://doi.org/10.3390/rs12071070.

Nguyen, N.L., Anger, J., Davy, A., Arias, P., Facciolo, G., 2021. Self-supervised multi-image super-resolution for push-frame satellite images. In: Presented at the Proceedings of the IEEE/CVF Conference on Computer Vision and Pattern Recognition, pp. 1121–1131.

Nieto, J.I., Monteiro, S.T., Viejo, D., 2010. 3D geological modelling using laser and hyperspectral data. In: in: 2010 IEEE International Geoscience and Remote Sensing Symposium. Presented at the 2010 IEEE International Geoscience and Remote Sensing Symposium, pp. 4568–4571. https://doi.org/10.1109/IGARSS.2010.5651553.

Nishar, A., Richards, S., Breen, D., Robertson, J., Breen, B., 2016. Thermal infrared imaging of geothermal environments and by an unmanned aerial vehicle (UAV): a case study of the Wairakei – Tauhara geothermal field, Taupo, New Zealand. Renew. Energy 86, 1256–1264. https://doi.org/10.1016/j.renene.2015.09.042.

Oyallon, E., Rabin, J., 2015. An analysis of the SURF method. Image Process. Line 5, 176–218.

Pádua, L., Guimarães, N., Adão, T., Sousa, A., Peres, E., Sousa, J.J., 2020. Effectiveness of Sentinel-2 in Multi-Temporal Post-Fire Monitoring When Compared with UAV Imagery. ISPRS Int. J. Geo-Inf. 9, 225. https://doi.org/10.3390/ijgi9040225.

Pádua, L., Marques, P., Adão, T., Guimarães, N., Sousa, A., Peres, E., Sousa, J.J., 2019. Vineyard variability analysis through UAV-based vigour maps to assess climate change impacts. Agronomy 9, 581. https://doi.org/10.3390/agronomy9100581.

Pádua, L., Vanko, J., Hruška, J., Adão, T., Sousa, J.J., Peres, E., Morais, R., 2017. UAS, sensors, and data processing in agroforestry: a review towards practical applications. Int. J. Remote Sens. 38, 2349–2391. https://doi.org/10.1080/01431161.2017.1297548.

Paul, S., Pati, U.C., 2021. A comprehensive review on remote sensing image registration. Int. J. Remote Sens. 42, 5396–5432. https://doi.org/10.1080/01431161.2021.1906985.

Pires, R.d.P., Olofsson, K., Persson, H.J., Lindberg, E., Holmgren, J., 2022. Individual tree detection and estimation of stem attributes with mobile laser scanning along boreal forest roads. ISPRS J. Photogramm. Remote Sens. 187, 211–224. https://doi.org/10.1016/j.isprsjprs.2022.03.004.

Poblete, T., Camino, C., Beck, P.S.A., Hornero, A., Kattenborn, T., Saponari, M., Boscia, D., Navas-Cortes, J.A., Zarco-Tejada, P.J., 2020. Detection of Xylella fastidiosa infection symptoms with airborne multispectral and thermal imagery: assessing bandset reduction performance from hyperspectral analysis. ISPRS J. Photogramm. Remote Sens. 162, 27–40.

Poblete, T., Navas-Cortes, J.A., Camino, C., Calderon, R., Hornero, A., Gonzalez-Dugo, V., Landa, B.B., Zarco-Tejada, P.J., 2021. Discriminating Xylella fastidiosa from Verticillium dahliae infections in olive trees using thermal- and hyperspectral-based plant traits. ISPRS J. Photogramm. Remote Sens. 179, 133–144. https://doi.org/10.1016/j.isprsjprs.2021.07.014.

Pôças, I., Calera, A., Campos, I., Cunha, M., 2020. Remote sensing for estimating and mapping single and basal crop coefficientes: a review on spectral vegetation indices approaches. Agric. Water Manag. 233, 106081.

Qadeer, M.U., Saeed, S., Taj, M., Muhammad, A., 2021. Spatio-temporal Crop Classification On Volumetric Data. ArXiv210310050 Cs.

Qian, G., Abualshour, A., Li, G., Thabet, A., Ghanem, B., 2021. Pu-gcn: Point cloud upsampling using graph convolutional networks. In: in: Proceedings of the IEEE/CVF Conference on Computer Vision and Pattern Recognition, pp. 11683–11692.

Qin, R., 2019. A critical analysis of satellite stereo pairs for digital surface model generation and a matching quality prediction model. ISPRS J. Photogramm. Remote Sens. 154, 139–150. https://doi.org/10.1016/j.isprsjprs.2019.06.005.

Qiu, L., Jing, L., Hu, B., Li, H., Tang, Y., 2020. A new individual tree crown delineation method for high resolution multispectral imagery. Remote Sens. 12, 585.

Qiu, R., Miao, Y., Zhang, M., Li, H., 2021. Detection of the 3D temperature characteristics of maize under water stress using thermal and RGB-D cameras. Comput. Electron. Agric. 191, 106551 https://doi.org/10.1016/j.compag.2021.106551.

Quattrochi, D.A., Luvall, J.C., 1999. Thermal infrared remote sensing for analysis of landscape ecological processes: methods and applications. Landsc. Ecol. 14, 577–598. https://doi.org/10.1023/A:1008168910634.

Rahlf, J., Breidenbach, J., Solberg, S., Næsset, E., Astrup, R., 2017. Digital aerial photogrammetry can efficiently support large-area forest inventories in Norway. For. Int. J. For. Res. 90, 710–718. https://doi.org/10.1093/forestry/cpx027.

Rapaka, A., Ramu, A., 2021. In: Multispectral Data Processing for Agricultural Applications Using Deep Learning Classification Methods. Springer International Publishing, Cham, pp. 63–82. https://doi.org/10.1007/978-3-030-47560-4_6.

Regaieg, O., Yin, T., Malenovský, Z., Cook, B.D., Morton, D.C., Gastellu-Etchegorry, J.-P., 2021. Assessing impacts of canopy 3D structure on chlorophyll fluorescence radiance and radiative budget of deciduous forest stands using DART. Remote Sens. Environ. 265, 112673 https://doi.org/10.1016/j.rse.2021.112673.

Rohith, G., Kumar, L.S., 2020. Super-resolution based deep learning techniques for panchromatic satellite images in application to pansharpening. IEEE Access 8, 162099–162121. https://doi.org/10.1109/ACCESS.2020.3020978.

Roscher, R., Behmann, J., Mahlein, A.-K., Dupuis, J., Kuhlmann, H., Plümer, L., 2016. Detection of Disease Symptoms on Hyperspectral 3D Plant Models. In: ISPRS Annals of the Photogrammetry, Remote Sensing and Spatial Information Sciences. Presented at the XXIII ISPRS Congress, Commission VII (Volume III-7) - 12–19 July 2016, Prague, Czech Republic, Copernicus GmbH, pp. 89–96. https://doi.org/10.5194/isprs-annals-III-7-89-2016.

Rothermel, M., Gong, K., Fritsch, D., Schindler, K., Haala, N., 2020. Photometric multi-view mesh refinement for high-resolution satellite images. ISPRS J. Photogramm. Remote Sens. 166, 52–62. https://doi.org/10.1016/j.isprsjprs.2020.05.001.

Ruiz, A.L., Rodríguez, J.M.J., Anguita, C.J.O., Higueruela, F.R.F., 2019. Multispectral Registration. Undistortion and Tree Detection for Precision Agriculture.

Rupnik, E., Pierrot-Deseilligny, M., Delorme, A., 2018. 3D reconstruction from multi-view VHR-satellite images in MicMac. ISPRS J. Photogramm. Remote Sens. 139, 201–211. https://doi.org/10.1016/j.isprsjprs.2018.03.016.

Saari, H., Akujärvi, A., Holmlund, C., Ojanen, H., Kaivosoja, J., Nissinen, A., Niemeläinen, O., 2017. Visible, very near IR and short wave IR hyperspectral drone imaging system for agriculture and natural water applicationS: Frontiers in Spectral imaging and 3D Technologies for Geospatial Solutions, ISPRS SPEC3D. In: Front. Spectr. Imaging 3D Technol. Geospatial Solut., International Archives of the

Photogrammetry, Remote Sensing and Spatial Information Sciences 165–170. https://doi.org/10.5194/isprs-archives-XLII-3-W3-165-2017.
Saarinen, N., Vastaranta, M., Näsi, R., Rosnell, T., Hakala, T., Honkavaara, E., Wulder, M. A., Luoma, V., Tommaselli, A.M.G., Imai, N.N., Ribeiro, E.A.W., Guimarães, R.B., Holopainen, M., Hyyppä, J., 2018. Assessing biodiversity in boreal forests with UAV-based photogrammetric point clouds and hyperspectral imaging. Remote Sens. 10, 338. https://doi.org/10.3390/rs10020338.
Sagan, V., Maimaitijiang, M., Bhadra, S., Maimaitiyiming, M., Brown, D.R., Sidike, P., Fritschi, F.B., 2021. Field-scale crop yield prediction using multi-temporal WorldView-3 and PlanetScope satellite data and deep learning. ISPRS J. Photogramm. Remote Sens. 174, 265–281. https://doi.org/10.1016/j.isprsjprs.2021.02.008.
Saleem, S., Sablatnig, R., 2014. A robust SIFT descriptor for multispectral images. IEEE Signal Process. Lett. 21, 400–403.
Sankey, J.B., Sankey, T.T., Li, J., Ravi, S., Wang, G., Caster, J., Kasprak, A., 2021. Quantifying plant-soil-nutrient dynamics in rangelands: Fusion of UAV hyperspectral-LiDAR, UAV multispectral-photogrammetry, and ground-based LiDAR-digital photography in a shrub-encroached desert grassland. Remote Sens. Environ. 253, 112223 https://doi.org/10.1016/j.rse.2020.112223.
Sankey, T., Donager, J., McVay, J., Sankey, J.B., 2017. UAV lidar and hyperspectral fusion for forest monitoring in the southwestern USA. Remote Sens. Environ. 195, 30–43. https://doi.org/10.1016/j.rse.2017.04.007.
Sankey, T.T., McVay, J., Swetnam, T.L., McClaran, M.P., Heilman, P., Nichols, M., 2018. UAV hyperspectral and lidar data and their fusion for arid and semi-arid land vegetation monitoring. Remote Sens. Ecol. Conserv. 4, 20–33.
Saralioglu, E., Gungor, O., 2020. Semantic segmentation of land cover from high resolution multispectral satellite images by spectral-spatial convolutional neural network. Geocarto Int. 1–21. https://doi.org/10.1080/10106049.2020.1734871.
Schiefer, F., Kattenborn, T., Frick, A., Frey, J., Schall, P., Koch, B., Schmidtlein, S., 2020. Mapping forest tree species in high resolution UAV-based RGB-imagery by means of convolutional neural networks. ISPRS J. Photogramm. Remote Sens. 170, 205–215. https://doi.org/10.1016/j.isprsjprs.2020.10.015.
Sedaghat, A., Mohammadi, N., 2019. High-resolution image registration based on improved SURF detector and localized GTM. Int. J. Remote Sens. 40, 2576–2601. https://doi.org/10.1080/01431161.2018.1528402.
Shen, X., Cao, L., Yang, B., Xu, Z., Wang, G., 2019. Estimation of Forest Structural Attributes Using Spectral Indices and Point Clouds from UAS-Based Multispectral and RGB Imageries. Remote Sens. 11, 800. https://doi.org/10.3390/rs11070800.
Sledz, A., Unger, J., Heipke, C., 2018. Thermal IR imaging: Image quality and orthophoto generation. Int. Arch. Photogramm. Remote Sens. Spat. Inf. Sci. - ISPRS Arch. 42 2018 Nr 1 42, 413–420. https://doi.org/10.15488/4082.
Sothe, C., Dalponte, M., de Almeida, C.M., Schimalski, M.B., Lima, C.L., Liesenberg, V., Miyoshi, G.T., Tommaselli, A.M.G., 2019. Tree species classification in a highly diverse subtropical forest integrating UAV-based photogrammetric point cloud and hyperspectral data. Remote Sens. 11, 1338. https://doi.org/10.3390/rs11111338.
Stojcsics, D., Lovas, I., Domozi, Z., Molnar, A., 2018. High Resolution 3D Thermal Imaging Using FLIR DUO R Sensor. In: Presented at the INES 2018 - IEEE 22nd International Conference on Intelligent Engineering Systems, pp. 000311–000316. https://doi.org/10.1109/INES.2018.8523914.
Stucker, C., Schindler, K., 2022. ResDepth: A deep residual prior for 3D reconstruction from high-resolution satellite images. ISPRS J. Photogramm. Remote Sens. 183, 560–580. https://doi.org/10.1016/j.isprsjprs.2021.11.009.
Su, Y., Guo, Q., Xue, B., Hu, T., Alvarez, O., Tao, S., Fang, J., 2016. Spatial distribution of forest aboveground biomass in China: estimation through combination of spaceborne lidar, optical imagery, and forest inventory data. Remote Sens. Environ. 173, 187–199. https://doi.org/10.1016/j.rse.2015.12.002.
Terentev, A., Dolzhenko, V., Fedotov, A., Eremenko, D., 2022. Current state of hyperspectral remote sensing for early plant disease detection: a review. Sensors 22, 757. https://doi.org/10.3390/s22030757.
Teza, G., Pesci, A., 2019. Evaluation of the temperature pattern of a complex body from thermal imaging and 3D information: a method and its MATLAB implementation. Infrared Phys. Technol. 96, 228–237. https://doi.org/10.1016/j.infrared.2018.11.029.
Torabzadeh, H., Morsdorf, F., Schaepman, M.E., 2014. Fusion of imaging spectroscopy and airborne laser scanning data for characterization of forest ecosystems – A review. ISPRS J. Photogramm. Remote Sens. 97, 25–35. https://doi.org/10.1016/j.isprsjprs.2014.08.001.
Torresan, C., Berton, A., Carotenuto, F., Gennaro, S.F.D., Gioli, B., Matese, A., Miglietta, F., Vagnoli, C., Zaldei, A., Wallace, L., 2017. Forestry applications of UAVs in Europe: a review. Int. J. Remote Sens. 38, 2427–2447. https://doi.org/10.1080/01431161.2016.1252477.
Truong, T.P., Yamaguchi, M., Mori, S., Nozick, V., Saito, H., 2017. Registration of RGB and Thermal Point Clouds Generated by Structure From Motion. In: in: 2017 IEEE International Conference on Computer Vision Workshops (ICCVW). Presented at the 2017 IEEE International Conference on Computer Vision Workshops (ICCVW), pp. 419–427. https://doi.org/10.1109/ICCVW.2017.57.
Tsai, C.-H., Lin, Y.-C., 2017. An accelerated image matching technique for UAV orthoimage registration. ISPRS J. Photogramm. Remote Sens. 128, 130–145. https://doi.org/10.1016/j.isprsjprs.2017.03.017.
Tsouros, D.C., Bibi, S., Sarigiannidis, P.G., 2019. A review on UAV-based applications for precision agriculture. Information 10, 349. https://doi.org/10.3390/info10110349.
Valbuena, R., 2014. Integrating Airborne Laser Scanning with Data from Global Navigation Satellite Systems and Optical Sensors. In: Maltamo, M., Næsset, E., Vauhkonen, J. (Eds.), Forestry Applications of Airborne Laser Scanning: Concepts and Case Studies, Managing Forest Ecosystems. Springer, Netherlands, Dordrecht, pp. 63–88. https://doi.org/10.1007/978-94-017-8663-8_4.
Valbuena, R., Hernando, A., Manzanera, J.A., Martínez-Falero, E., García-Abril, A., Mola-Yudego, B., 2018. Most similar neighbor imputation of forest attributes using metrics derived from combined airborne LIDAR and multispectral sensors. Int. J. Digit. Earth 11, 1205–1218. https://doi.org/10.1080/17538947.2017.1387183.
Vanegas, F., Bratanov, D., Powell, K., Weiss, J., Gonzalez, F., 2018. A novel methodology for improving plant pest surveillance in vineyards and crops using UAV-based hyperspectral and spatial data. Sensors 18, 260. https://doi.org/10.3390/s18010260.
Villacrés, J., Auat Cheein, F.A., 2022. Construction of 3D maps of vegetation indices retrieved from UAV multispectral imagery in forested areas. Biosyst. Eng. 213, 76–88. https://doi.org/10.1016/j.biosystemseng.2021.11.025.
Vollmer, M., Möllmann, K., 2017. Infrared Thermal Imaging: : Fundamentals, Research and Applications. Wiley. https://doi.org/10.1002/9783527693306.ch3.
Vong, A., Matos-Carvalho, J.P., Toffanin, P., Pedro, D., Azevedo, F., Moutinho, F., Garcia, N.C., Mora, A., 2021. How to build a 2d and 3d aerial multispectral map?—all steps deeply explained. Remote Sens. 13 https://doi.org/10.3390/rs13163227.
Wachs, J.P., Stern, H.I., Burks, T., Alchanatis, V., 2010. Low and high-level visual feature-based apple detection from multi-modal images. Precis. Agric. 11, 717–735. https://doi.org/10.1007/s11119-010-9198-x.
Wan, H., Tang, Y., Jing, L., Li, H., Qiu, F., Wu, W., 2021. Tree species classification of forest stands using multisource remote sensing data. Remote Sens. 13, 144.
Wang, X., Li, P., 2020. Extraction of urban building damage using spectral, height and corner information from VHR satellite images and airborne LiDAR data. ISPRS J. Photogramm. Remote Sens. 159, 322–336. https://doi.org/10.1016/j.isprsjprs.2019.11.028.
Webster, C., Westoby, M., Rutter, N., Jonas, T., 2018. Three-dimensional thermal characterization of forest canopies using UAV photogrammetry. Remote Sens. Environ. 209, 835–847. https://doi.org/10.1016/j.rse.2017.09.033.
Weiser, F., Baumann, E., Jentsch, A., Medina, F.M., Lu, M., Nogales, M., Beierkuhnlein, C., 2022. Impact of Volcanic Sulfur Emissions on the Pine Forest of La Palma. Spain. Forests 13, 299. https://doi.org/10.3390/f13020299.
Westfeld, P., Mader, D., Maas, H.-G., 2015. Generation of TIR-attributed 3D Point Clouds from UAV-based Thermal Imagery. Photogramm. - Fernerkund. - Geoinformation 381–393. https://doi.org/10.1127/1432-8364/2015/0274.
Wulder, M.A., Loveland, T.R., Roy, D.P., Crawford, C.J., Masek, J.G., Woodcock, C.E., Allen, R.G., Anderson, M.C., Belward, A.S., Cohen, W.B., 2019. Current status of Landsat program, science, and applications. Remote Sens. Environ. 225, 127–147.
Xu, R., Li, C., Bernardes, S., 2021. Development and testing of a UAV-based multi-sensor system for plant phenotyping and precision agriculture. Remote Sens. 13, 3517. https://doi.org/10.3390/rs13173517.
Yandun Narvaez, F., Reina, G., Torres-Torriti, M., Kantor, G., Cheein, F.A., 2017. A Survey of Ranging and Imaging Techniques for Precision Agriculture Phenotyping. IEEEASME Trans. Mechatron. 22, 2428–2439. https://doi.org/10.1109/TMECH.2017.2760866.
Yao, H., Qin, R., Chen, X., 2019. Unmanned aerial vehicle for remote sensing applications—A Review. Remote Sens. 11, 1443. https://doi.org/10.3390/rs11121443.
Yeo, S., Lafon, V., Alard, D., Curti, C., Dehouck, A., Benot, M.-L., 2020. Classification and mapping of saltmarsh vegetation combining multispectral images with field data. Estuar. Coast. Shelf Sci. 236, 106643 https://doi.org/10.1016/j.ecss.2020.106643.
Yu, R., Luo, Y., Zhou, Q., Zhang, X., Wu, D., Ren, L., 2021. Early detection of pine wilt disease using deep learning algorithms and UAV-based multispectral imagery. For. Ecol. Manag. 497, 119493.
Yuan, W., Choi, D., 2021. UAV-Based Heating Requirement Determination for Frost Management in Apple Orchard. Remote Sens. 13, 273. https://doi.org/10.3390/rs13020273.
Yue, J., Feng, H., Jin, X., Yuan, H., Li, Z., Zhou, C., Yang, G., Tian, Q., 2018. A Comparison of crop parameters estimation using images from UAV-mounted snapshot hyperspectral sensor and high-definition digital camera. Remote Sens. 10, 1138. https://doi.org/10.3390/rs10071138.
Zainuddin, K., Majid, Z., Ariff, M.F.M., Idris, K.M., Abbas, M.A., Darwin, N., 2019. 3D Modeling for rock art documentation using lightweight multispectral camera. Int. Arch. Photogramm. Remote Sens. Spat. Inf. Sci.
Zarco-Tejada, P.J., Camino, C., Beck, P.S.A., Calderon, R., Hornero, A., Hernández-Clemente, R., Kattenborn, T., Montes-Borrego, M., Susca, L., Morelli, M., Gonzalez-Dugo, V., North, P.R.J., Landa, B.B., Boscia, D., Saponari, M., Navas-Cortes, J.A., 2018. Previsual symptoms of Xylella fastidiosa infection revealed in spectral plant-trait alterations. Nat. Plants 4, 432–439. https://doi.org/10.1038/s41477-018-0189-7.
Zhang, B., Zhao, L., Zhang, X., 2020. Three-dimensional convolutional neural network model for tree species classification using airborne hyperspectral images. Remote Sens. Environ. 247, 111938 https://doi.org/10.1016/j.rse.2020.111938.
Zhang, R., Li, G., Li, M., Wang, L., 2018. Fusion of images and point clouds for the semantic segmentation of large-scale 3D scenes based on deep learning. ISPRS J. Photogramm. Remote Sens. 143, 85–96. https://doi.org/10.1016/j.isprsjprs.2018.04.022.
Zhang, Y., Yang, W., Sun, Y., Chang, C., Yu, J., Zhang, W., 2021. Fusion of multispectral aerial imagery and vegetation indices for machine learning-based ground classification. Remote Sens. 13, 1411.
Zheng, H., Zhong, X., Yan, J., Zhao, L., Wang, X., 2020. A thermal performance detection method for building envelope based on 3d model generated by UAV thermal imagery. Energies 13. https://doi.org/10.3390/en13246677.
Zhou, Z., Majeed, Y., Diverres Naranjo, G., Gambacorta, E.M.T., 2021. Assessment for crop water stress with infrared thermal imagery in precision agriculture: a review and future prospects for deep learning applications. Comput. Electron. Agric. 182, 106019 https://doi.org/10.1016/j.compag.2021.106019.

Zhu, J., Xu, Y., Hoegner, L., Stilla, U., 2019. Direct co-registration of TIR images and MLS point clouds by corresponding keypoints. In: Presented at the ISPRS Annals of the Photogrammetry, Remote Sensing and Spatial Information Sciences, pp. 235–242. https://doi.org/10.5194/isprs-annals-IV-2-W7-235-2019.

Zhu, J., Xu, Y., Ye, Z., Hoegner, L., Stilla, U., 2021. Fusion of urban 3D point clouds with thermal attributes using MLS data and TIR image sequences. Infrared Phys. Technol. 113, 103622 https://doi.org/10.1016/j.infrared.2020.103622.

Zia, A., Liang, J., Zhou, J., Gao, Y., 2015. 3D Reconstruction from Hyperspectral Images. In: 2015 IEEE Winter Conference on Applications of Computer Vision. Presented at the 2015 IEEE Winter Conference on Applications of Computer Vision, pp. 318–325. https://doi.org/10.1109/WACV.2015.49.